Fusion of Inertial Sensors and
Orthogonal Frequency Division Multiplexed (OFDM)
Signals of Opportunity
for Unassisted Navigation

THESIS

Capt. Jason G. Crosby,

AFIT/GE/ENG/09-11

DEPARTMENT OF THE AIR FORCE
AIR UNIVERSITY

AIR FORCE INSTITUTE OF TECHNOLOGY

Wright-Patterson Air Force Base, Ohio

AFIT/GE/ENG/09-11

Fusion of Inertial Sensors and
Orthogonal Frequency Division Multiplexed (OFDM)
Signals of Opportunity
for Unassisted Navigation

THESIS

Presented to the Faculty

Department of Electrical and Computer Engineering

Graduate School of Engineering and Management

Air Force Institute of Technology

Air University

Air Education and Training Command

In Partial Fulfillment of the Requirements for the

Degree of Master of Science in Electrical Engineering

Capt. Jason G. Crosby, B.S.E.E.

March 2009

APPROVED FOR PUBLIC RELEASE; DISTRIBUTION UNLIMITED.

AFIT/GE/ENG/09-11

Fusion of Inertial Sensors and Orthogonal Frequency Division Multiplexed (OFDM) Signals of Opportunity for Unassisted Navigation

Capt. Jason G. Crosby, B.S.E.E.

Approved:

/signed/	10 Mar 2009
Dr. Richard Martin (Chairman)	date
/signed/	10 Mar 2009
Dr. John Raquet (Member)	date
/signed/	10 Mar 2009
LtCol. Michael Veth, PhD (Member)	date

AFIT/GE/ENG/09-11

Abstract

The advent of the global positioning system (GPS) has provided worldwide high-accuracy position measurements. However, GPS may be rendered unavailable by jamming, disruption of satellites, or simply by signal shadowing in urban environments. Thus, this thesis considers fusion of Inertial Navigation Systems (INS) and Orthogonal Frequency Division Multiplexed (OFDM) signals of opportunity (SOOP) for navigation. Typical signal of opportunity navigation involves the use of a reference receiver and uses time difference of arrival (TDOA) measurements. However, by exploiting the block structure of OFDM communication signals, the need for the reference receiver is reduced or possibly removed entirely. This research uses a Kalman Filter (KF) to optimally combine INS measurements with the OFDM TDOA measurements. A proof of concept in two dimensions is shown, and effects of the number of transmitters, sampling rate, multipath, and clock errors are investigated.

Acknowledgements

First and foremost I would like to thank my thesis advisor, Dr. Richard Martin. Without his guidance and support throughout this research effort I would not have been able to complete it. The technical expertise and advice were insightful, motivational, and greatly appreciated.

I would also like to thank all of my friends in the Comm\RADAR lab. Their company made the long days bearable.

Finally I would like to thank my wife for her support. Her love and understanding was the only thing that kept me sane throughout this whole process.

Capt. Jason G. Crosby

Table of Contents

List of Figures

List of Tables

List of Abbreviations

FUSION OF INERTIAL SENSORS AND

ORTHOGONAL FREQUENCY DIVISION MULTIPLEXED (OFDM)

SIGNALS OF OPPORTUNITY

FOR UNASSISTED NAVIGATION

I. Introduction

This chapter describes the problem to be addressed by this research. Background of the problem and goals for this research are given, as well as assumptions used to limit the scope of the research. Previous related research is provided as well as the organization for the rest of the thesis.

1.1 Background

The *Global Positioning System* (GPS) has emerged all over the world as the number one system used for precise navigation. However, there are many places where the use of GPS may be denied or its accuracy may be degraded. Such areas include urban cities, where tall buildings may block a line of sight path to the satellites; while others include hostile battlefield areas where an enemy may employ a GPS jamming device. With these potential problems with GPS a reliable backup precision navigation system is needed. While *Inertial Navigation Systems* (INS) have been researched thoroughly, high accuracy systems remain much too expensive for use in many applications. Lower quality INS systems exist but are only accurate for a short time, thus an additional system must be used to improve the quality during extended use.

One potential type of non-GPS navigation is navigation via *Signals of Opportunity* (SOOP). SOOP are defined as radio frequency signals that were not originally intended to be used for navigation, but could be exploited and used to aid navigation. Such signals include but are not limited to AM and FM radio, broadcast television

signals, cellular communications, and broadcast multicarrier systems. While cellular communication towers are often very dense in urban areas yielding many SOOPs, many of these systems use GPS for time synchronization. This means that when GPS is unavailable, precise navigation using these signals may not be possible [6]. Previous research has investigated AM, FM, and television signals for their navigation potential and found promising results [6], [9], [11]. However, these systems employ single carrier modulation and could be subject to unwanted multipath effects (see Section 2.3). Given that one of the major areas of concern is urban areas, another option needs to be found.

One subset of multicarrier systems is *Orthogonal Frequency Division Multiplexed* (OFDM) systems. OFDM signals are used in systems such as *Digital Video Broadcast* (DVB), *Digital Audio Broadcast* (DAB), and wireless *Local Area Networks* (LAN) [19] making them very abundant in urban areas. In addition to being very widespread, OFDM systems have many advantages that make them suitable for use in navigation. Many OFDM systems are broadcast from the Earth's surface as opposed to being broadcast from a satellite in space. To ensure the signals reach everyone intended many groundstations broadcast the same signal. Finally the OFDM signal has a well defined block structure. This structure may allow for the removal of the reference receiver typically needed when calculating a receiver's position.

1.2 Research Goals

The primary goal of this research is to prove the concept that OFDM signals can be used to aid an *Inertial Navigation System* (INS) through the use of a *Kalman Filter* (KF). The use of OFDM signals will also be shown to reduce the bandwidth needed by a *Reference Receiver* (RR) or possibly remove the reference receiver entirely. Furthermore effects of the number of transmitters used, oversampling of the transmitters, multipath, and transmitter clock errors are investigated.

1.3 Assumptions

For this research, the following assumptions were made:

- The OFDM signals have an established infrastructure around the area of interest

- The signals operate within the frequency range of the receivers

- The signals possess a known modulation and signal structure (OFDM)

- Signal transmitter locations are known

- The INS can be initialized (i.e. initial position is known)

- Initial transmitter locations with respect to the receiver are known

1.4 Related Research

This section describes *Time Difference of Arrival* (TDOA) navigation sysems, as well as several non-TDOA navigation systems including *Received Signal Strength* (RSS), *Time of Arrival* (TOA), and *Angle of Arrival* (AOA). Finally some previous work using OFDM signals of opportunity for navigation is presented.

1.4.1 TDOA-based Navigation Systems. TDOA measurements can be taken two ways. First, two transmitters can transmit the same signal at the same time. One receiver can then calculate the difference in arival times for each signal. The other way uses one transmitter and two receivers. One receiver is refered to as the reference and is at a known location and does not move. The other known as the mobile moves and is the receiver whose position needs to be found. The receivers each calculate the arival time of the signal from the transmitter. The reference receiver then sends the arrival time it calculated to the mobile receiver. The mobile receiver can then find a TDOA measurement between the two and calculate its position. This technique is more common, because in most cases two transmitters broadcasting the same signal simultaneously are not available. This technique is illustrated in Figure 1.1 [16]. The *Long Range Navigation* (Loran) system currently uses this type of measurement [12].
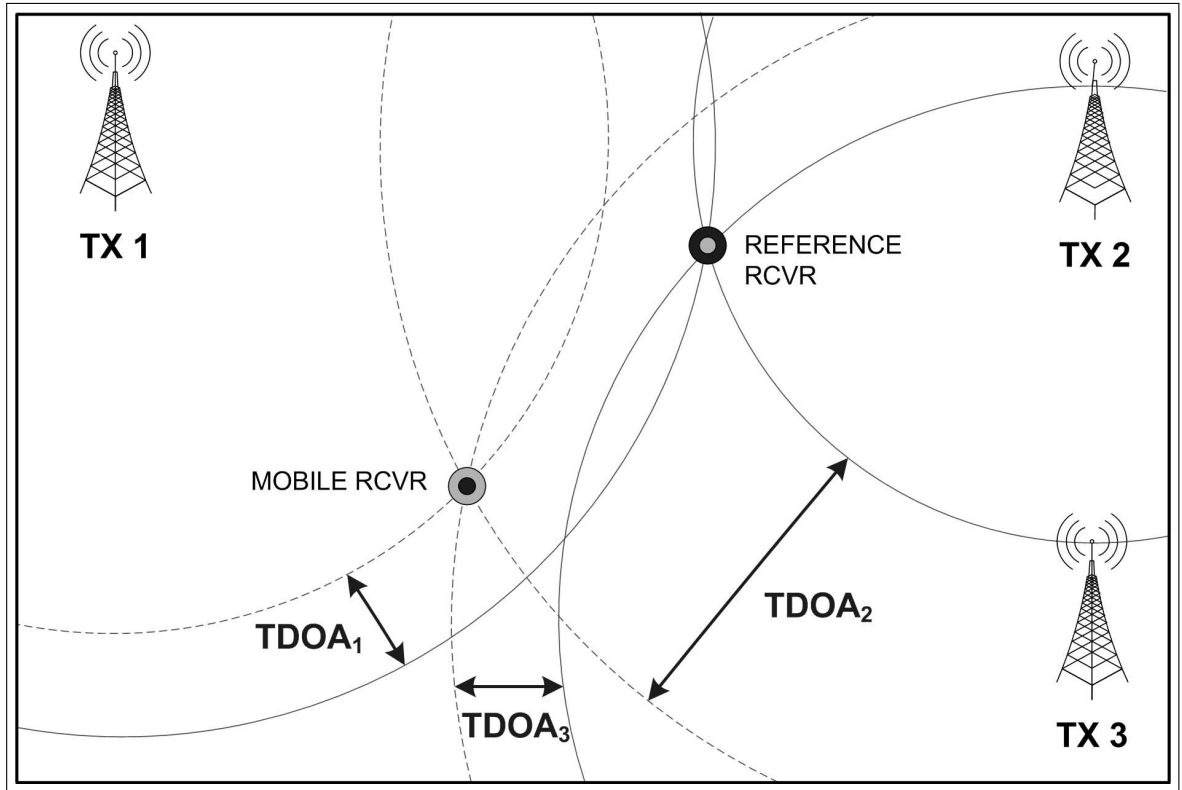
Figure 1.1:   TDOA measurement using a reference receiver. [16]

1.4.2   Non-TDOA-based Navigation Systems.   Typical non-TDOA-based position estimation methods include:

- RSS

- TOA

- AOA

RSS This method uses a known mathematical model describing the path loss attenuation with distance [5]. This will estimate a distance D between the transmitter and receiver. This distance gives a circle with radius D around the transmitter, which the receiver must be on. With multiple transmitters an intersection of multiple circles can be found thus giving the position of the receiver. Multipath errors are the dominant source of errors in this type of measurement, but the use of more measurements may help position accuracy.
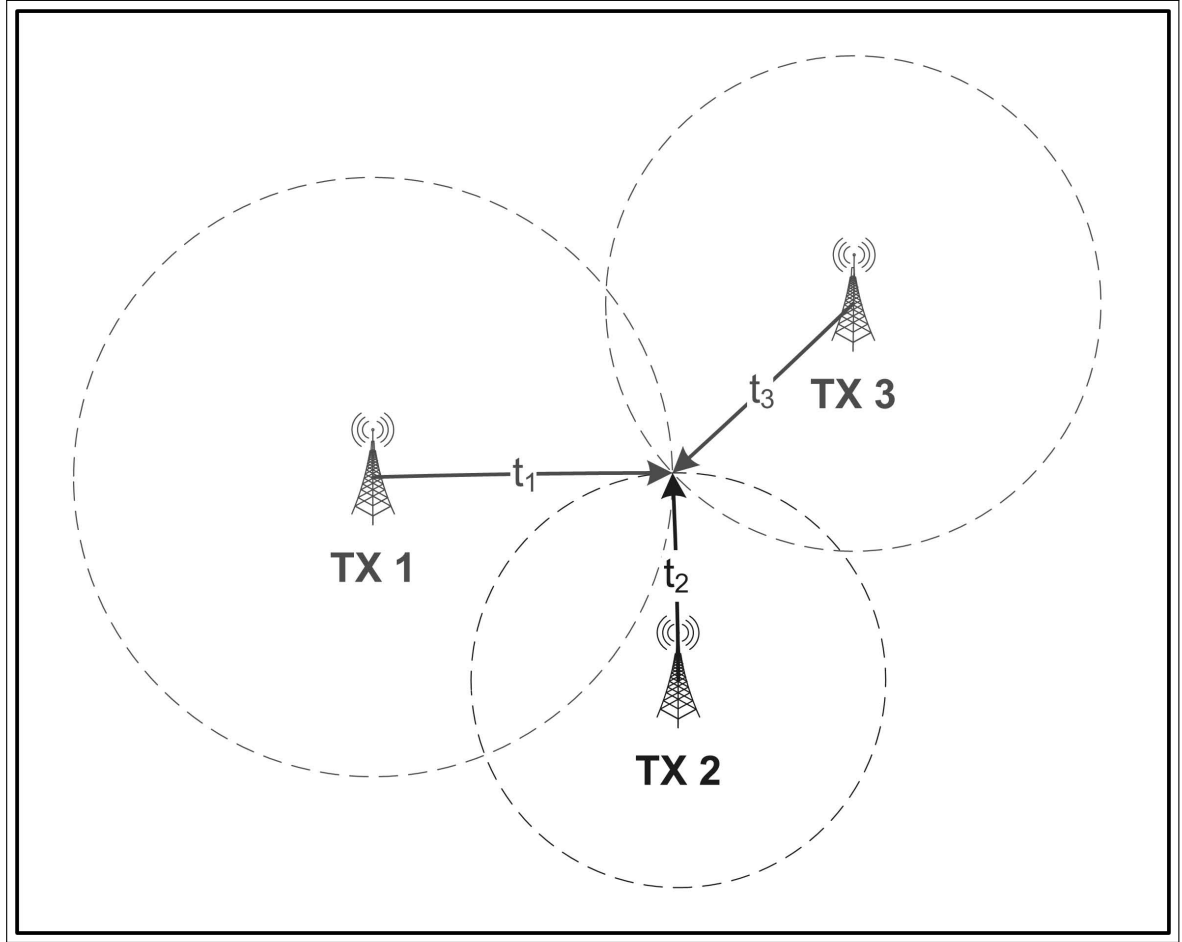
Figure 1.2:   TOA measurement. The position is calculated by finding the distance between transmitter and receiver. [16]

TOA This method finds the distance between the transmitter and receiver by finding the one way propogation time between the transmitter and receiver [5]. As in RSS this puts the receiver on a circle around the transmitter. Position is then found in the same way as RSS. Errors can occur when the transmitters are not synchronized. When the transmitters are synchronized the receiver clock error is the same for all measurements and be calculated, thus giving accurate measurements. This technique is illustrated in Figure 1.2 [16].

AOA This method uses antenna arrays to measure the angle to a transmitter with a known location [5]. This puts the receiver on a line passing through the transmitter. With additional measurements an intersection of multiple lines can be
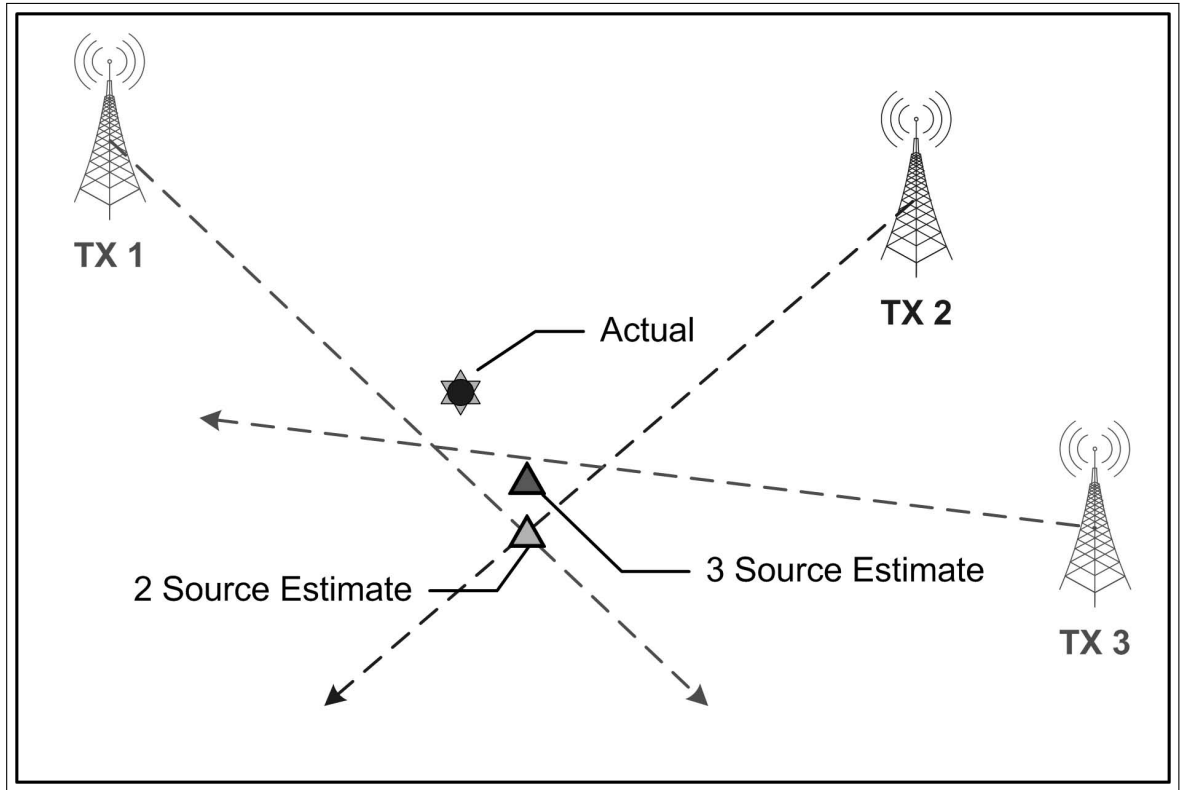
Figure 1.3:   AOA measurement. The position is calculated by finding the direction to the transmitter. [16]

found thus giving position. Using more than two sources can increase accuracy, but AOA measurements are much less accurate over long distances. As a receiver moves farther away from the transmitters the position accuracy will decrease. This technique is illustrated in Figure 1.3 [16].

1.4.3   Previous OFDM SOOP Research.   Previous research using OFDM signals of opportunity has shown that the inherent block structure of the signal can be exploited to obtain TDOA measurements [16]. Exploiting this block structure also allows for smaller bandwidth requirements between the reference and mobile receivers. The block structure allows for individual symbols to be distinguished. Statistics such as mean or variance for each symbol can be calculated at the reference receiver. These statistics can then be transmitted from the reference to the mobile receiver and correlated with statistics calculated at the mobile receiver. By correlating the string

of statistics a TDOA can be found. In non-OFDM systems, the entire signal must be retransmitted from the reference to the mobile and then correlated. A significant amount of bandwidth is saved by only transmitting one statistic per symbol rather than the entire symbol.

1.5   Thesis Organization

Chapter II provides a description of the OFDM signal structure, TDOA calculation algorithms, multipath, INS model, and Kalman Filter. *Chapter III* explains the methodology used in this research, and various simulations conducted. *Chapter IV* details the results from the simulations described in *Chapter III*. Finally, *Chapter V* gives a summary of the research and lists conclusions of the thesis as well as potential follow-on research areas.

II. Background

This chapter provides the technical background necessary for understanding the overall concepts of this research. A description of the OFDM signal structure is provided along with the TDOA computation algorithm. An overview of multipath is presented, and an explanation of a basic INS is given. Finally the operation of a Kalman Filter is presented.

2.1 OFDM Signals

OFDM is a communication technique where multiple subcarriers are chosen so that each subcarrier is orthogonal to every other subcarrier. For the subcarriers to be orthogonal the following must be true:

$$\int_0^{n \cdot T} x_1(f) \cdot x_2^*(f) \cdot df = 0, \ n = 1, 2, 3, \dots \tag{2.1}$$

where T is the period of the signal, x_1 and x_2 are input signals, and $*$ represents the complex conjugate operation.

A block diagram of an OFDM transmitter is shown in Figure 2.1. The first step in OFDM transmission occurs at the bit level. Information bits are encoded and then go through an interleaving process. This is followed by constellation mapping then an *Inverse Fast Fourier Transform* (IFFT) is performed. This output goes through a *Parallel to Serial* (P/S) converter , and finally a *cyclic prefix* (CP) is added.

2.1.1 Coding. Channel coding refers to the class of signal transformations designed to improve communications performance by enabling the transmitted signals to better withstand the effects of various channel impairments, such as noise, interference, and fading [14]. OFDM systems such as LANs typically use convolutional encoding [1] while trellis coded modulation along with frequency and time interleaving has been proven to be very effective [20].
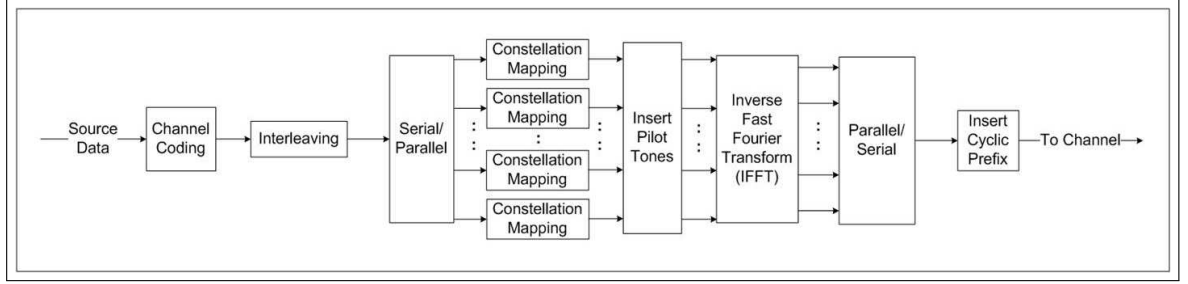
Figure 2.1: OFDM transmitter block diagram. After coding and interleaving, bits to be transmitted are mapped using a signal constellation onto multiple carrier frequencies. An IFFT is then performed on the carrier frequencies. Once in the time domain a cyclic prefix is added and the symbol is transmitted over the channel.

2.1.2 Interleaving. When coding is used to improve bit error rate in communication systems they typically only work for up to a specified number of errors per symbol. For example a system may be able to correct all bit errors as long as there are no more than 3 bit errors per symbol. However, if the communication channel is temporarily degraded significantly, this may cause a string of errors back to back. This could potentially cause more errors than the coding can correct, resulting in incorrect decoding. By interleaving bits the errors are spread out among multiple symbols. If spread out enough the total number of errors per symbol will be within the correction threshold of the code. Thus correct decoding of the bits will occur.

2.1.3 Constellation Mapping. Once coding and interleaving are finished the serial bit stream is divided into N parrallel bit streams, where N is the symbol length. Once in parallel, bits from each stream are mapped onto a signal constellation. Typical modulation types are *Binary Phase Shift Keying* (BPSK), *Quadriture Phase Shift Keying* (QPSK), and *M-ary Quadriture Amplitude Modulation* (M-QAM). For this research the data was mapped to a QPSK constellation which can be seen in figure 2.2.

2.1.4 IFFT. After encoded bits are mapped to a signal constellation an IFFT is performed. An IFFT takes the modulated data (which is in the frequency

9
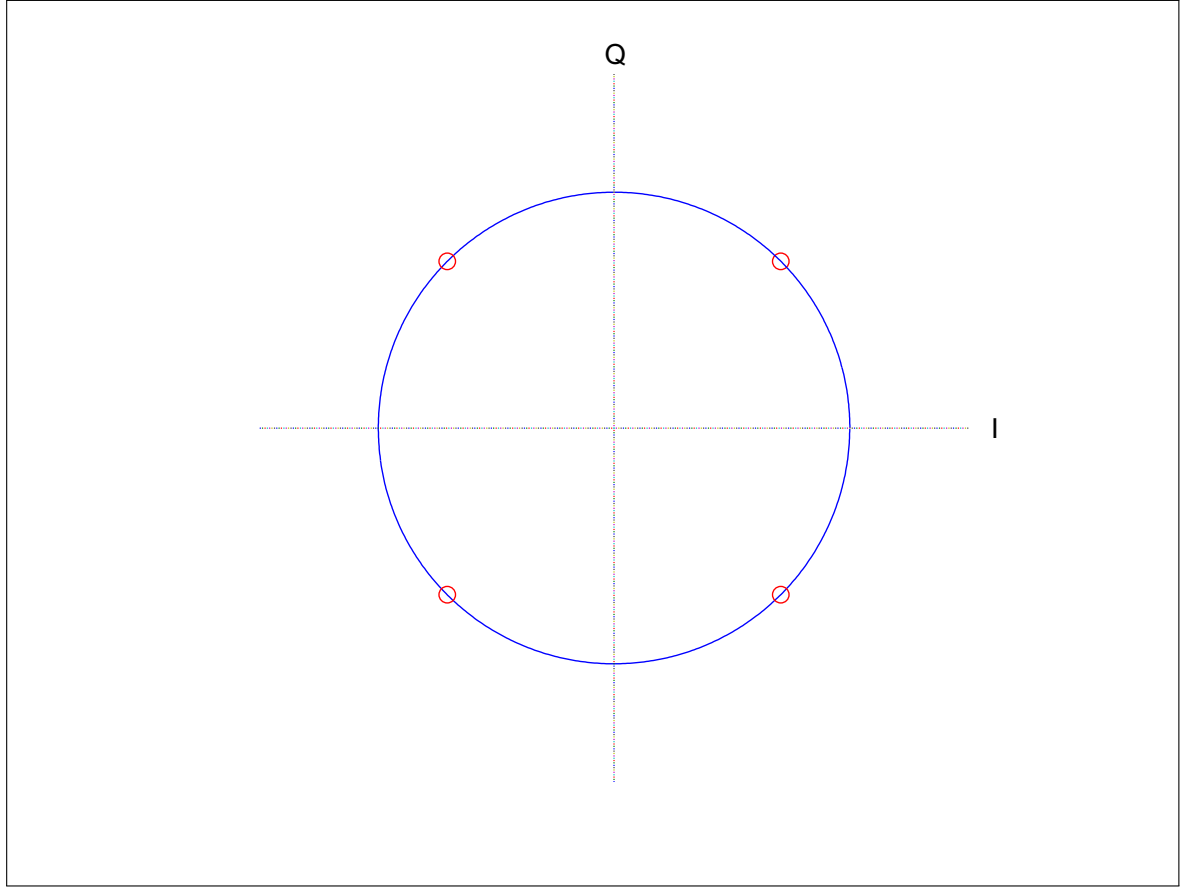
Figure 2.2:   QPSK Signal Constellation

domain) and transforms it to the time domain. This operation is accomplished via
the formula

$$x_s(n) = \frac{1}{N} \cdot \sum_{k=0}^{N-1} S_s(k) \cdot W_N^{-k \cdot n}, \ n = 0, 1, \ldots, N-1 \qquad (2.2)$$

where

$$W_N = e^{-\frac{j \cdot (2\pi)}{N}} \qquad (2.3)$$

and $S_s(k)$ is the kth sample of the sth frequency domain data symbol, and $x_s(n)$ is
the nth sample of the sth time domain symbol. Variables n and k range from 0 to
$N-1$. Once the IFFT is performed there will be N parallel time domain samples.
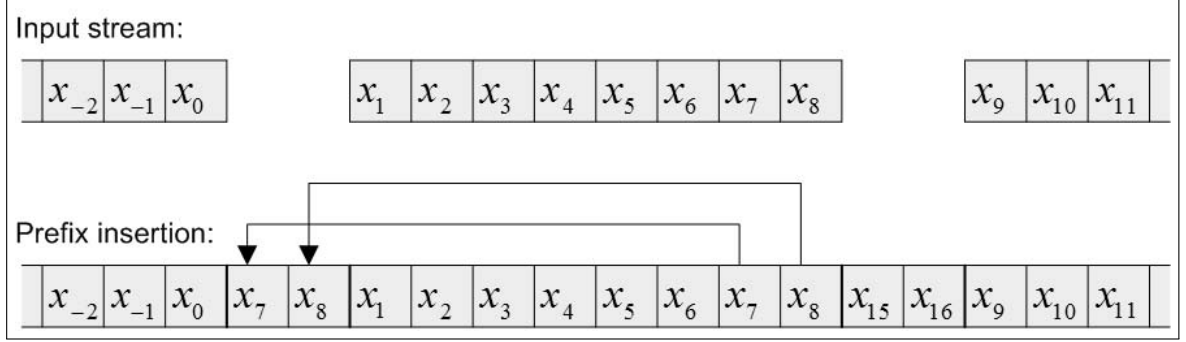
Figure 2.3: Insertion of Cyclic Prefix. v samples are copied from the end of each symbol and appended to the front of the symbol.

These samples must be taken from parallel to a serial sample stream. Once in serial, the CP is added.

2.1.5 Cyclic Prefix. After the IFFT is performed, the last v samples of the symbol are copied and appended to the beginning of the symbol. This makes the symbol to be transmitted $N + v$ samples long. This is graphically represented in figure 2.3. This is done in order to mitigate the effects of *Inter Symbol Interference* (ISI), and *Inter Channel Interference* (ICI). The CP can be viewed as a guard band, and as long as any multipath delays are smaller than the CP length any distortion of the signal will be contained in the CP. This distortion can later be removed by the OFDM receiver [18].

2.2   TDOA Calculation

In this section we discuss how TDOA measurements are obtained from the OFDM signals. The geometry for this problem is shown in figure 2.4. Unlike the two methods of TDOA calculation described in section (1.4), this TDOA calculation method uses a single transmitter and a single receiver to take a self TDOA measurement. An example of the self TDOA measurement is shown in figure 2.5

In order to perform a self TDOA measurement, the first step is to estimate an initial block boundary within the signal. This is a common method of blind

11
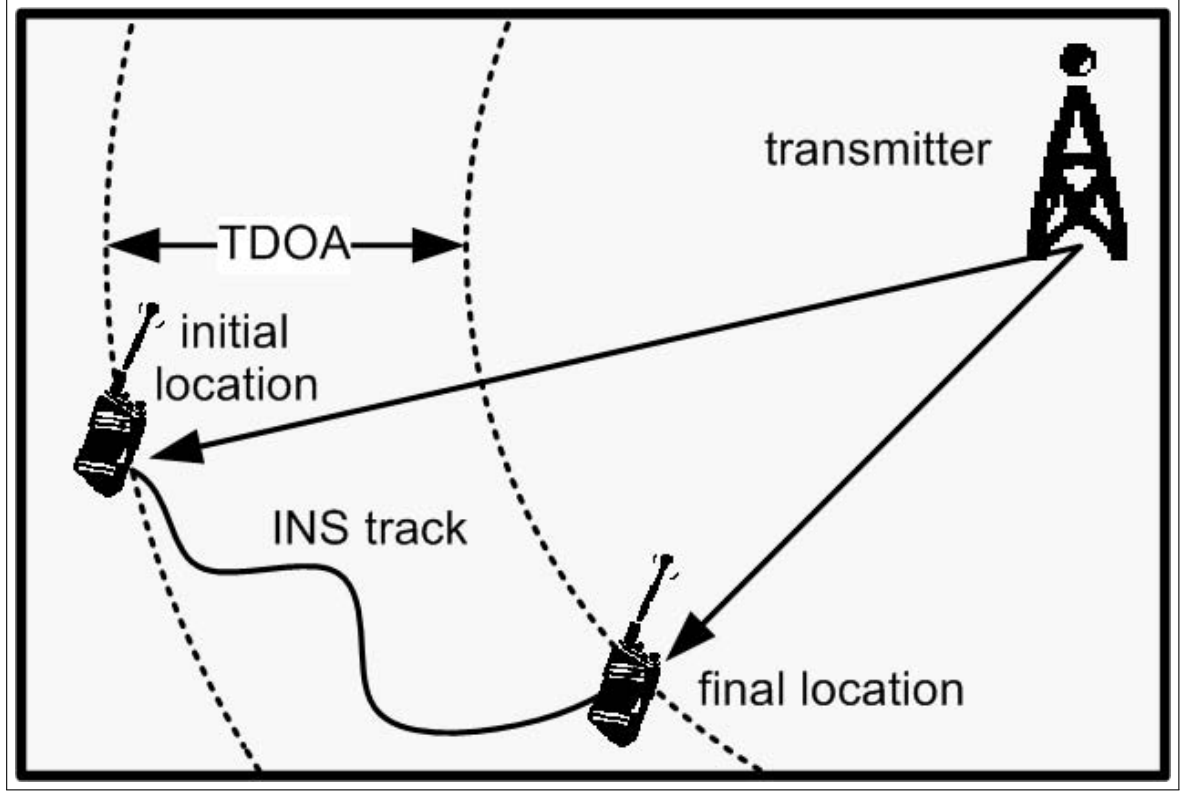
Figure 2.4: TDOA calculation model used in this research. Block boundries are estimated at two different times. TDOA is calculated by differencing the block boundries.

block synchronization and is derived in [2]. Once block boundaries are estimated an average boundary estimate over multiple symbols formulated in [16] is taken. Thus given a received signal y_{rx} the maximum likelihood (ML) estimate of the initial block boundary $\delta_{initial}$ position is

$$\hat{\delta}_{initial} = \arg \max_{0 \leq m \leq M-1} \Re\{\gamma_{avg}(m)\} \tag{2.4}$$

where

$$\gamma_{avg}(m) = \sum_{k=0}^{K-1} \sum_{i=m+1}^{m+v} y_{rx}(Mk+i)y_{rx}^*(Mk+i+N) \tag{2.5}$$

and $\Re$ is the real operator, K is the number of blocks averaged over, M is the symbol length, k is the index of the OFDM block, and i is the index of the sample within
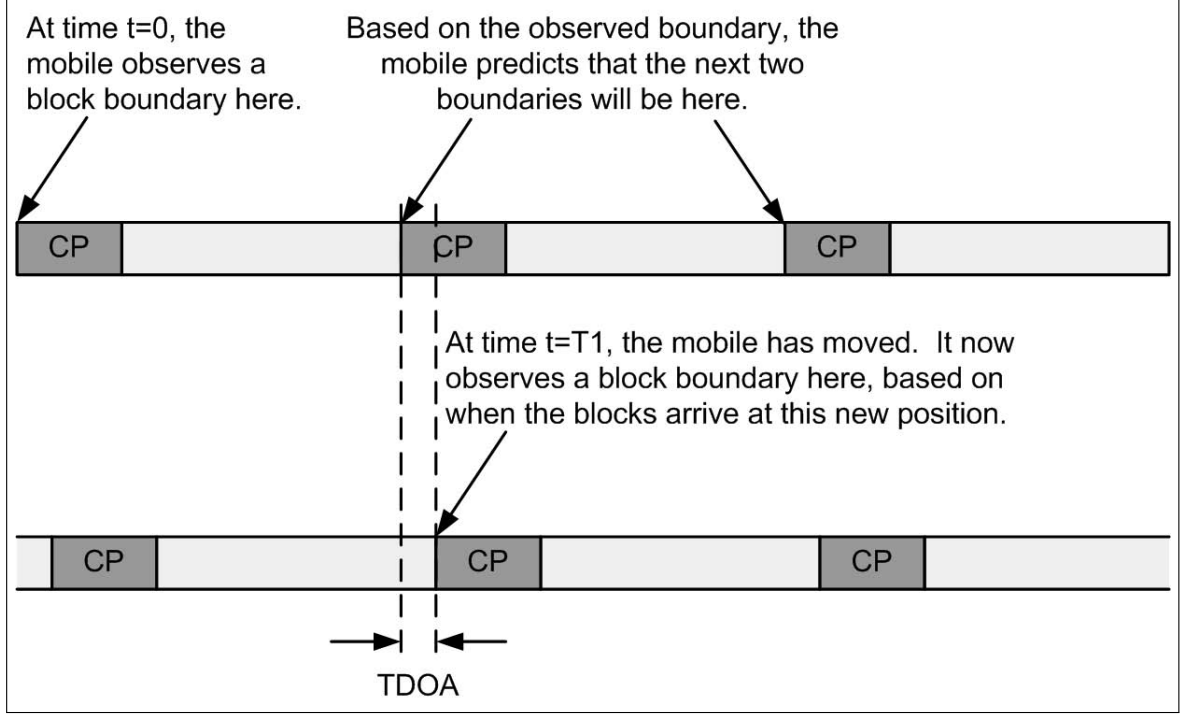
Figure 2.5:   A pictoral example of the self TDOA computation. Block boundary times are predicted and compared to actual block boundary times.

the OFDM block. Once the initial block boundary is found the system can then predict when a block boundary should occur in the future. Because there are an integer number of symbols between each time a measurement is taken the predicted block boundary is the same as $\delta_{initial}$. As the receiver moves time goes by and the receiver will encounter these boundaries. However, because the receiver has moved the actual boundary position will be slightly earlier if the receiver has moved toward the transmitter, or slightly later if the receiver has moved away from the transmitter. This new measured block boundary position $\hat{\delta}_{ML,rx}$ is calculated the same way as $\delta_{initial}$. Finally, once $\hat{\delta}_{ML,rx}$ is obtained the TDOA can be calculated using the formula

$$TDOA = (\hat{\delta}_{ML,rx} - \delta_{initial}) \cdot T_s \qquad (2.6)$$

where T_s is the sampling interval. Note that in these simulations $\delta_{initial}$ is always zero, and all TDOA measurements are measured from the initial point (0,0).

2.3 Multipath

Multipath occurs when there is more than one path for the signal between transmitter and receiver [4]. In an urban environment these multiple paths are typically caused by reflection from buildings and other structures in the environment or even reflection from the atmosphere. Typically the line of sight path from the transmitter to the receiver is the strongest and most dominant path, but that is not always the case. If the line of sight path is obscured a multipath signal may become dominant. Typically many multipath signals with different delays are experienced and these signals may add constructively or destructively. The impact these multipath signals may have depends on many factors such as their power relative to that of the dominant path, and range of delays.

2.4 Inertial Navigation Systems

This section describes the operation of a simple two dimensional INS system used in this research. A more rigorous three dimensional model can be found in [15]. An INS uses two types of measurement devices: accelerometers to measure specific force, and gyroscopes to measure rotation angle, or angular rotation rate. These measurements are then resolved into the navigation frame and integrated to obtain position information.

2.4.1 Accelerometers. Accelerometers are used to measure specific force. Specific force is usually defined as the sum of acceleration (a) and gravity (g). Einstein theorized that these two forces are indistinguishable and thus can only be measured together [7]. In this research the effects of gravity are neglected and the accelerometers are assumed to measure only acceleration. Units of this measurement are $\frac{meters}{second^2}$. Two accelerometers were used; one initially pointing in the X direction (f_{xb}) and the other initially pointing in the Y direction (f_{yb}). Accelerometer measurements are affected by various types of errors including but not limited to: bias, alignment errors, and
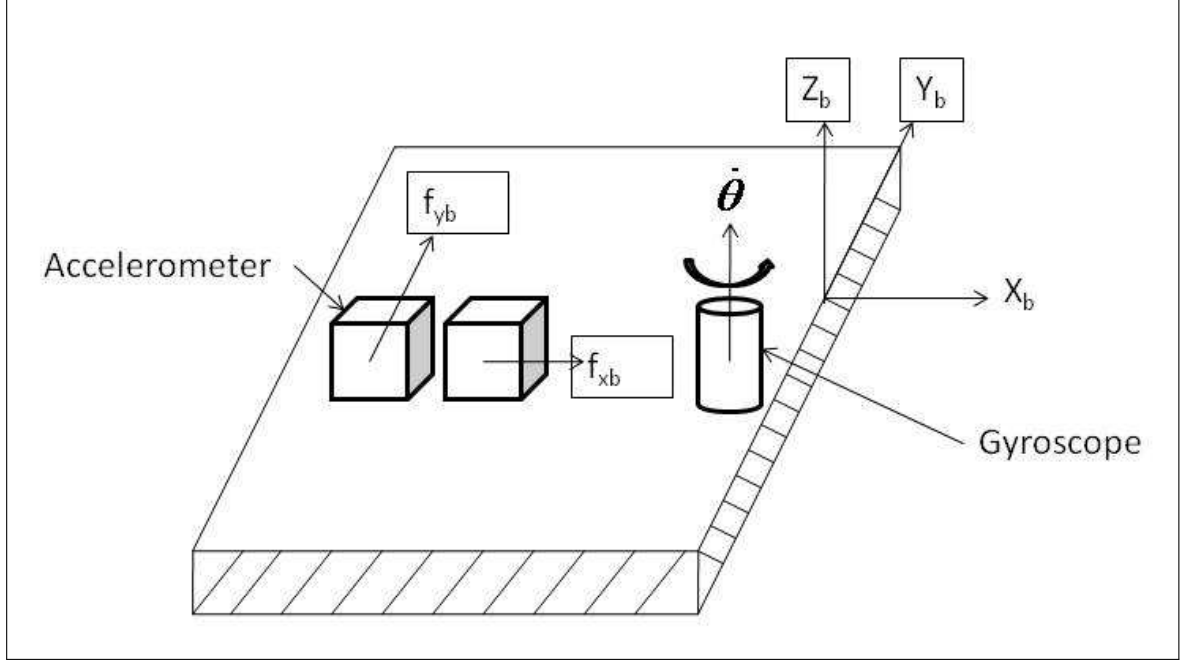
Figure 2.6: INS model used in the simulation. A two dimensional model with two accelerometers and one gyroscope. Position is obtained in the X and Y directions.

noise. To simulate some of these effects *Additive White Gaussian Noise* (AWGN) was added to all simulated measurements which will be discussed in Chapter 3.

2.4.2 Gyroscopes. Gyroscopes are used to measure rotation angle or angular rotation rate. For this research gyroscopes were used to measure angular rate. Units of this measurement are $\frac{radians}{second}$. One gyroscope was used with the rotation axis in the Z direction ($\dot{\Theta}$). Gyroscope measurements are affected by various types of errors including but not limited to: bias, alignment errors, and noise. To simulate some of these effects AWGN was added to all simulated measurements which will be discussed in Chapter 3.

2.4.3 Obtaining Position. The full system used to obtain position information is shown in figure 2.6. The body accelerations were resolved in the X and Y directions using the formulas found in [15] which are:

$$\Theta\left(t\right) = \int_0^t \dot{\Theta}\left(\tau\right) + w_1 d\tau + \Theta\left(o\right) \tag{2.7}$$

$$f_{xi} = \left(f_{xb} + w_2\right) \cdot \cos(\Theta) + \left(f_{yb} + w_3\right) \cdot \sin(\Theta) \tag{2.8}$$

$$f_{yi} = -\left(f_{xb} + w_2\right) \cdot \sin(\Theta) + \left(f_{yb} + w_3\right) \cdot \cos(\Theta) \tag{2.9}$$

where f_{xb} and f_{yb} are measured acceleration in the X_b and Y_b body frame. Accelerations f_{xi} and f_{yi} are resolved in the X and Y directions. Varibles w_1, w_2, and w_3 are AWGN noise sources discussed in detail in Chapter 3. INS measurements for this research were taken at 50Hz. X and Y position were then obtained via the formulas:

$$v_{xi}\left(t\right) = \int_0^t f_{xi}\left(\tau\right) d\tau + v_{xi}\left(0\right) \tag{2.10}$$

$$v_{yi}\left(t\right) = \int_0^t f_{yi}\left(\tau\right) d\tau + v_{yi}\left(0\right) \tag{2.11}$$

$$X\left(t\right) = \int_0^t v_{xi}\left(\tau\right) d\tau + X\left(0\right) \tag{2.12}$$

$$Y\left(t\right) = \int_0^t v_{yi}\left(\tau\right) d\tau + Y\left(0\right) \tag{2.13}$$

Although the AWGN added to the simulated measurements was zero mean, these errors cause an error drift due to the fact that they are integrated twice. This causes errors in INS position solution to grow over time. Because of these continuously growing errors, INS systems are typically aided by some sort of measurement system. Here we will use OFDM signals of opportunity to aid the INS system through the use of a Kalman filter.
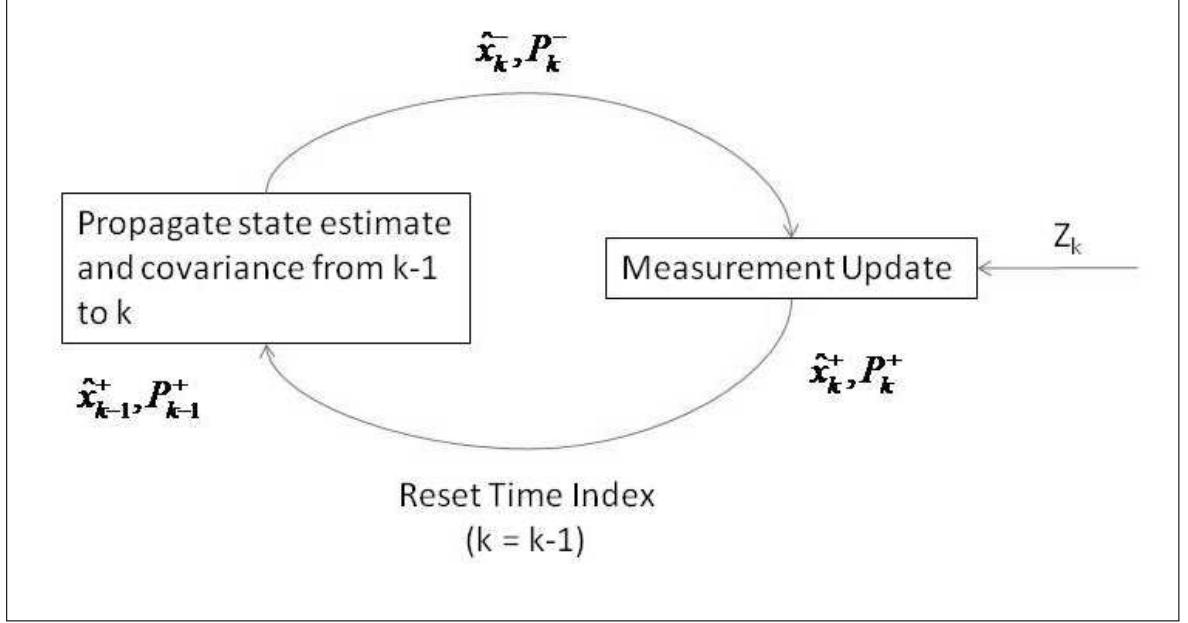
Figure 2.7:   Kalman Filter. Recursive data processing algorithm.

2.5   *Kalman Filter*

A Kalman Filter is an optimal recursive data processing algorithm [10]. More simply it provides optimal estimates of a system state. This recursive process is shown in Figure 2.7 [3]. Because inputs to the KF are all time varying and contain errors a perfect estimate is unobtainable. Instead the Kalman filter provides a probability density function of the output. Because the KF assumes all errors have a Gaussian distribution, this can be done by keeping track of two things: the state mean and covariance. This operation has two steps: state propogation and measurement updating.

2.5.1   State Propogation.   Given a stochastic difference equation

$$x_k = \Phi_{k-1}x_{k-1} + B_{k-1}u_{k-1} + w_{k-1} \tag{2.14}$$

where x is a state vector, Φ is the state transition matrix, B is the input matrix, and w is the additive noise vector, state estimates can be propogated with the formulas:

$$\widehat{x_k^-} = \Phi_{k-1}\widehat{x_{k-1}^+} + B_{k-1}u_{k-1} \tag{2.15}$$

$$P_k^- = \Phi_{k-1}P_{k-1}^+\Phi_{k-1}^T + Q_{k-1} \tag{2.16}$$

where P is the covariance matrix, Q is the covariance of w, a superscript $-$ denotes time just prior to a measurement update, and a superscript $+$ denotes time just after a measurement update.

2.5.2 Measurement Update. Once the state estimate and covariance have been propogated the measurement update step occurs. If there is in fact no measurement at that time the updates are simply:

$$\widehat{x_k^+} = \widehat{x_k^-} \tag{2.17}$$

$$P_k^+ = P_k^- \tag{2.18}$$

However, if a measurement is taken at time k given the measurement model

$$z_k = H_k x_k + v_k \tag{2.19}$$

where Z is the measurement taken by a sensor, H is the observation matrix relating the state vector to the measurement, and v is a zero mean noise vector with covariance R, the measurement update equations become:

$$\widehat{x_k^+} = \widehat{x_k^-} + K_k\left(Z_k - H_k\widehat{x_k^-}\right) \tag{2.20}$$

$$P_k^+ = (I - K_kH_k)\,P_k^- \tag{2.21}$$

18

where

$$K_k = P_k^- H_k^T \left[H_k P_k^- H_k^T + R_k \right]^{-1} \tag{2.22}$$

The matrix product $H_k \widehat{x_k^-}$ is the predicted measurement based on the current state of the filter. The difference between this and the actual measurement Z is known as the residual. The Kalman Gain K relates how accurate the measurements are as opposed to the propogated states. If K is large, the filter will weight the measurements high, while a small K will weight measurements low.

2.5.3 Extended Kalman Filter.   The Kalman filter described in the previous section assumes a linear model driven by white Gaussian noise. However, sometimes systems are non-linear and an extended Kalman filter must be used. An extended Kalman filter still has the same two operations as the regular Kalman filter: state propogation and measurement update. The state propogation step uses the system model

$$\dot{x}(t) = f\left[x(t), u(t), t\right] + Gw(t) \tag{2.23}$$

With this new model the F, B, and G matrices may need to be calculated at each propogation step. Matrix multiplication cannot be used. Once these matrices have been calculated the propogation step occurs in the same manner as the regular Kalman filter.

The new measurement update model is

$$Z_k = h(x_k) + v_k \tag{2.24}$$

The extended Kalman filter assumes that over a small region of operation that the measurement model can be linearized. To linearize Equation (2.24) the partial derivitive of H with respect to each state is taken. This is effectively a first order

Taylor Series expansion of H. These partial derivitives evaluated at the current state vector then become elements of the H matrix used in Equation (2.20) through (2.22).

Because of the non linearity, the predicted measurement $H_k x_k$ cannot be obtained with matrix multiplication. Instead the function $h(x_k)$ must be used to calculate the predicted measurement. Once the predicted measurement has been calculated and the actual measurement Z has been taken, equations (2.20) through (2.22) are used to update the state estimates. Now that the measurement update has occured, the filter will continue to propogate the state estimates until another measurement occurs.

III. Research Methodology

This chapter describes the process used to perform proof of concept simulations. All simulations were developed using MATLAB. Simulating the INS measurements is presented along with the formulation of a truth reference. Obtaining the position estimate from the INS is described followed by a description of how the OFDM signals and TDOAs were generated. Derivation of the equations used by the Kalman Filter is presented followed by several different error sources that were incorpoted in later simulations. The final section describes different simulations that were conducted. These results will be the subject of chapter 4.

3.1 Simulating INS Measurements

In order to simulate INS measurements, first the time length for the simulation T was set. $T = 120s$ was used for all simulations. Using the model from figure 2.6, two body acceleration profiles f_{xb} and f_{yb} and one angular rate profile $\dot{\Theta}$ were generated. These profiles were generated at both 50 Hz and 1000 Hz. The 50 Hz profile would later be used for simulated INS measurements, while the much finer 1000 Hz would be used for a truth reference. The 50 Hz profiles can be seen in figure 3.1.

3.2 Truth Reference

In order to ensure that the Kalman filter was working a truth reference was needed. The 1000 Hz acceleration and angular rate profiles were used to generate this reference. First the rotation angle Θ had to be found. To do this numerical integration was performed on $\dot{\Theta}$ using the *cumtrapz* function. Once Θ was found the body accelerations could be resolved in the X and Y directions using equations (2.8) and (2.9). Once accelerations were resolved in the navigation frame they could be double integrated to obtain positions in the X and Y directions. These integrations were performed again using the *cumtrapz* function. The truth reference trajectory plot is shown in figure 3.2.
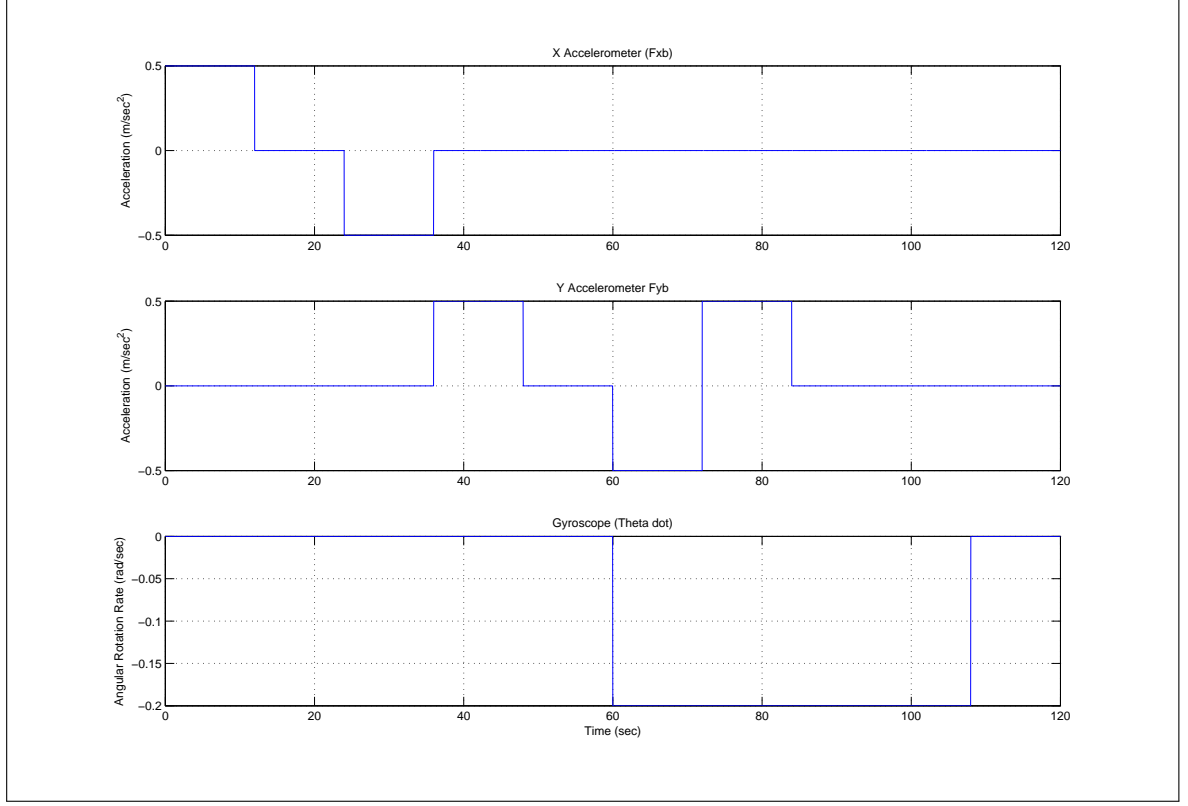
Figure 3.1:   50 Hz profiles for f_{xb}, f_{yb} and $\dot{\Theta}$

3.3   Obtaining Position Estimate from INS Measurements

The simulated INS was set to run at 50 Hz. In order to simulate INS measurements AWGN was added to f_{xb}, f_{yb}, and $\dot{\Theta}$. Noise for the accelerometers was zero mean with a standard deviation of $0.1\frac{m}{sec^2}$ and noise for the gyroscope was zero mean with a standard deviation of $0.1\frac{rad}{sec}$. The accelerometer standard deviation value used here is similar to that of the Microbotics, Inc *MIDG II* INS/GPS system noise standard deviation of $0.196\frac{m}{sec^2}$ which is used by the Air Force Institute of Technology's Advanced Navigation Technology Center for various tests. The gycoscope standard deviation value is significantly larger than that of the same system whos noise standard deviation is only $0.0087\frac{rad}{sec}$ [17]. Once AWGN was added, the INS estimated position was then calculated in the same way as the truth reference. The INS estimated trajectory is also shown in figure 3.2.

22
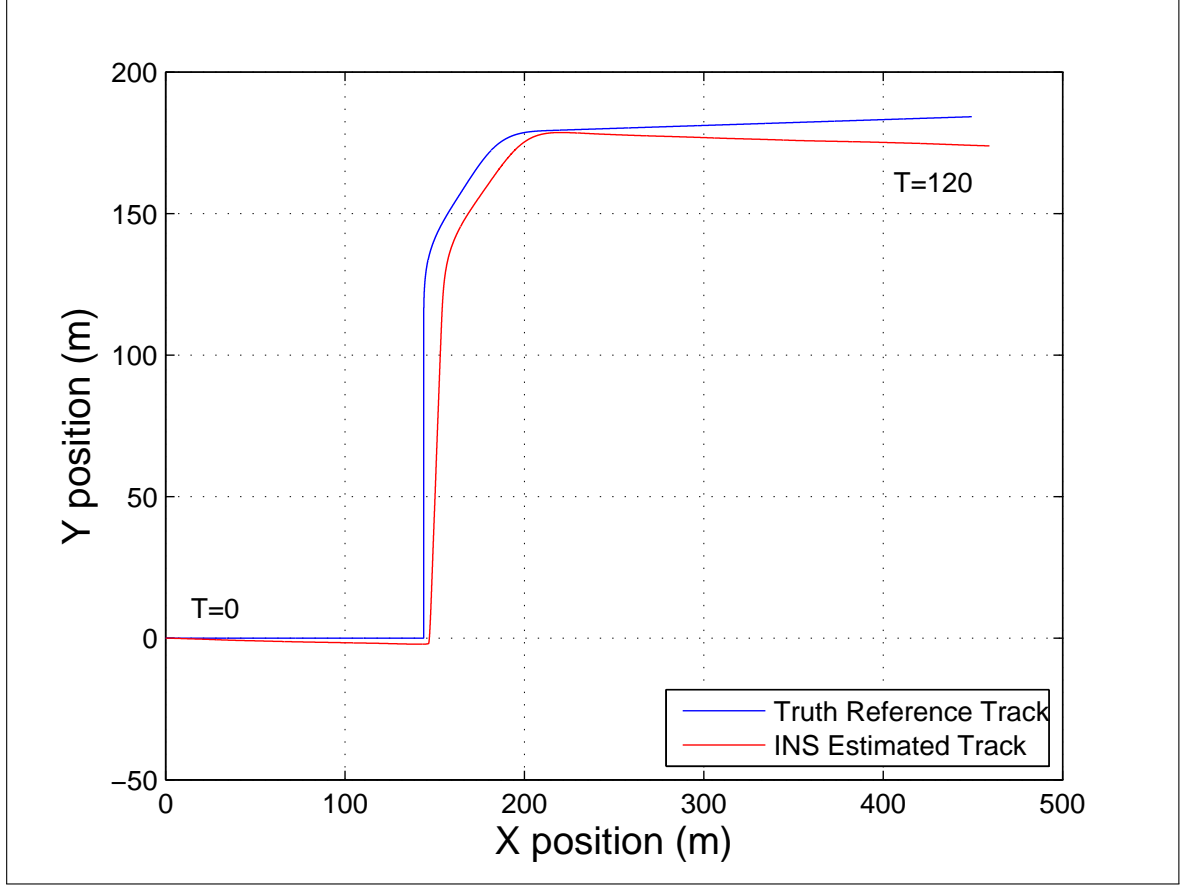
Figure 3.2:   Truth reference trajectory and INS estimated trajectory

3.4   Simulating OFDM Signals, Movement and Calculating TDOA Measurements

Because INS position errors grow over time, they are typically aided by another system in order to improve position accuracy. For this research OFDM SOOP are used. Three transmitters were used simulating three seperate SOOPs. Because the receiver initial position was assumed known and the position of the transmitters were assumed known the initial relative position between the receiver and transmitters is known. Therefor the navigation frame could be centered anywhere. For ease the navigation frame was chosen to be centered at the receiver initial position, and the initial receiver coordinates were (0,0). Three OFDM transmitters were then aranged in a triangular fashion around the receiver. This model is shown in figure 3.3.
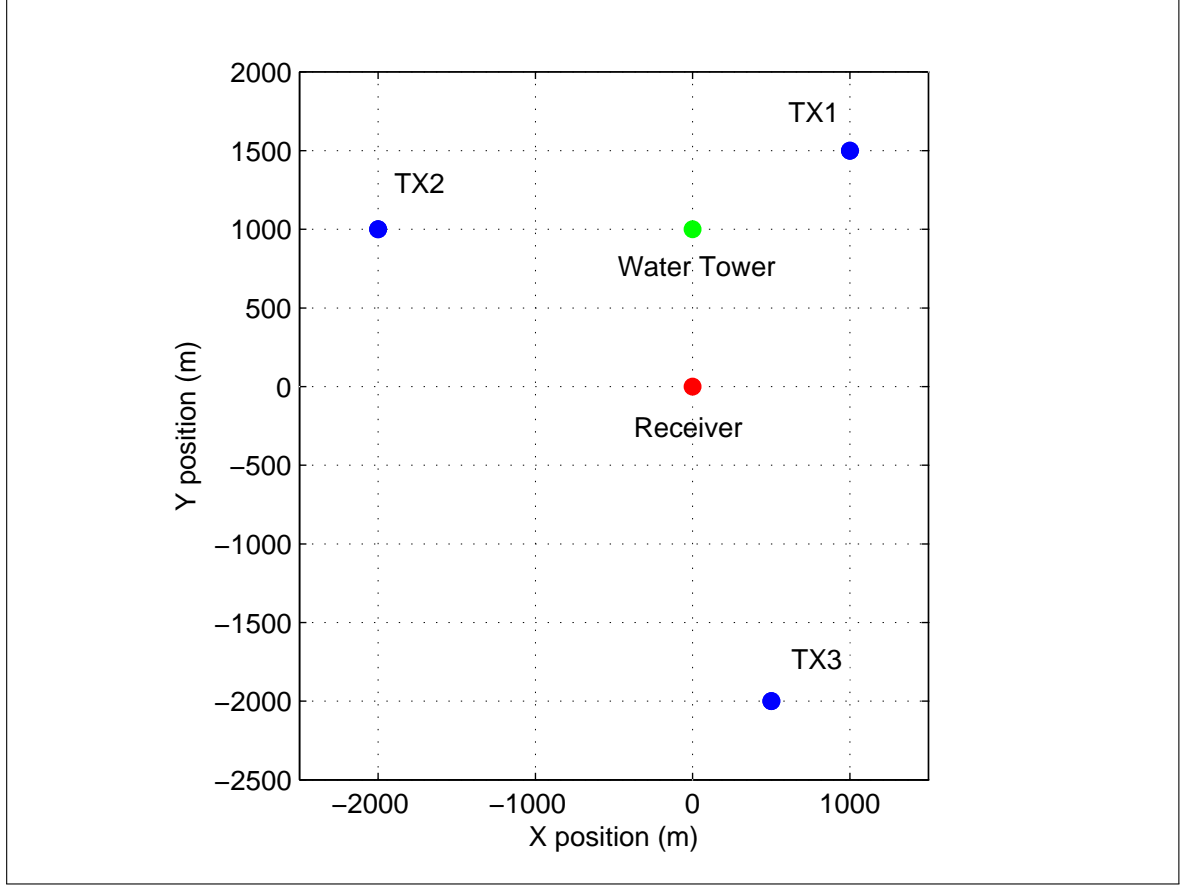
Figure 3.3: Receiver centered at (0,0) with transmitter 1 at (1000,1500), transmitter 2 at (-2000,1000), transmitter 3 at (500,-2000) and water tower at (0,1000). Note that poition coordinates are in meters from the reference.

To generate simulated OFDM signals, a function developed in [16] was modified and used. This function was capable of using QPSK, 16-QAM, or 64-QAM. For this research QPSK was used. This function produced a length L string of OFDM symbols. Each OFDM symbol had $N = 64$ information samples, and $v = 16$ cyclic prefix samples for a total of 80 samples in each OFDM Symbol. Bandwidth for each transmitter was 20 MHz, leaving the sampling interval at 50 nsec. This meant that each sample of the signal corresponded to a duration of approximately 15 meters. TDOA measurements were taken once per second. It has been shown in [16] that window size or the number of symbols used to calculate a TDOA can affect accuracy. If too large a window size is used the TDOA will not be approximately constant over

24

the window which can cause errors, while if too small a window size is used noise can affect accuracy more easily. For this research a total measurement time of 1 msec or $L = 250$ OFDM symbols was used each time a TDOA measurement was taken. TDOA measurements were taken once per second. The TDOA over this interval will be approximately constant and should combat noise effects.

Because there was no actual movement by the receiver, movement had to be simulated. To do this the truth reference (see section 3.2) was used to calculate how far the receiver had moved at each second where a TDOA measurement was taken. This could then be used to calculate the actual distance between the receiver and the transmitter at each second. By subtracting this from the initial distance to the transmitters the distance moved was found. Note that all these distances are in meters.

Once the amount of actual movement was known, the corresponding signal delay had to be simulated. To do this 1 extra OFDM symbol would have to be generated leaving $L = 251$. This string of OFDM symbols was then interpolated using the *interp* command. The string was interpolated by a factor of 15 so that each sample now corresponded to a duration of 1 meter. This string of OFDM symbols would then be *circshifted* a number of samples corresponding the amount of movement needing to be simulated. So to simulate movement each OFDM string of symbols with each sample corresponding to 1 meter was circshifted by floor (distance moved in meters).

By interpolating and then circshifting a finer movement can be simulated. If only the original 15 meter spaced samples were used, simulated movement resolution would only be 15 meters. Now simulated movement resolution is 1 meter. Using all the samples also allowed for a more accurate TDOA measurement. This is in effect a sampling frequency of 300 MHz. Simulations using this sampling frequency were conducted to determine the effect of oversampling the OFDM signals. However, this sampling frequency is very high and may not be feasible on a receiver. It was decided to see how well a lower sampling rate and less accurate TDOA measurements would

work. In order to simulate a 20 MHz sampling frequency only every fifteenth sample was used.

Finally once the OFDM signals were generated the TDOA was calculated using the process in section 2.2.

3.5   Aiding the INS through a Kalman Filter

This section describes the Kalman Filter propogation and measurement update steps.

3.5.1   Propogation.   Once a TDOA was obtained, a Kalman Filter was used to aid the INS and increase position accuracy. First, in order to obtain a difference equation to be used in the propogation step, a linear stochastic differential equation based on the INS model must be obtained in the form:

$$\dot{x} = Fx + B\left(t\right)u + G\left(t\right)w \tag{3.1}$$

where F is the system dynamics matrix, $B\left(t\right)$ is the input matrix, u is the input vector, $G\left(t\right)$ is the noise transformation matrix, and w is a vector of white noise. Note that $B\left(t\right)$ and $G\left(t\right)$ are time varying. Based on equations (2.8) through (2.13) the stochastic differential equation turns out to be

$$\begin{pmatrix} \dot{\Theta} \\ \ddot{X} \\ \ddot{Y} \\ \dot{X} \\ \dot{Y} \end{pmatrix} = \begin{pmatrix} 0 & 0 & 0 & 0 & 0 \\ 0 & 0 & 0 & 0 & 0 \\ 0 & 0 & 0 & 0 & 0 \\ 0 & 1 & 0 & 0 & 0 \\ 0 & 0 & 1 & 0 & 0 \end{pmatrix} \begin{pmatrix} \Theta \\ \dot{X} \\ \dot{Y} \\ X \\ Y \end{pmatrix} + \begin{pmatrix} 1 & 0 & 0 \\ 0 & cos(\Theta) & sin(\Theta) \\ 0 & -sin(\Theta) & cos(\Theta) \\ 0 & 0 & 0 \\ 0 & 0 & 0 \end{pmatrix} \begin{pmatrix} \dot{\Theta} \\ f_{xb} \\ f_{yb} \end{pmatrix}$$

$$+ \begin{pmatrix} 1 & 0 & 0 \\ 0 & cos(\Theta) & sin(\Theta) \\ 0 & -sin(\Theta) & cos(\Theta) \\ 0 & 0 & 0 \\ 0 & 0 & 0 \end{pmatrix} \begin{pmatrix} w_1 \\ w_2 \\ w_3 \end{pmatrix}$$

Once the stochastic differential equation has been formulated the stochastic difference equation can be obtained. First Φ_k from equation (2.14) is obtained by computing the matrix exponential of F

$$\Phi_k = e^{F \cdot dt} \tag{3.2}$$

where dt is the sampling interval for the INS. Because the INS sampling rate is 50 Hz, $dt = 0.02$. B_k can then be calculated symbolically using the equation

$$B_k = \int_0^{dt} e^{F \cdot (dt-\tau)} \cdot B d\tau \tag{3.3}$$

Once calculated symbolically, 0.02 is substituted for dt. Note that B_k changes every sample because of the dependence on Θ and must be calculated at every propogation step, while Φ_k is constant. Because the simulated INS measurements were

discrete, the variance of the AWGN added to the INS measurements is also the values on each diagonal element of the Q_k from equation 2.16 matrix leaving

$$Q_k = \begin{pmatrix} 0.01 & 0 & 0 \\ 0 & 0.01 & 0 \\ 0 & 0 & 0.01 \end{pmatrix}$$

Now that Φ_k, B_k, and Q_k are known, the propogation step of the Kalman Filter can occur using equations (2.15) and (2.16). This step will continue to occur fifty times per second until a discrete TDOA measurement is taken.

3.5.2 Measurement Update. In order to incorporate a TDOA update a measurement model must first be obtained. To do this the state vector x derived earlier must be related to the TDOA measurement ΔR. Because all the TDOA measurements are measuring the difference from the initial position, ΔR is the difference of the initial distance to the transmitter R_I and the current distance to the transmitter R_n where n is the transmitter number.

$$\Delta R_n = R_{I,n} - R_n \tag{3.5}$$

Because locations of the receiver initial position and transmitter are known R_I can be calculated [8].

$$R_{I,n} = \sqrt{(X_n - X_I)^2 + (Y_n - Y_I)^2} \tag{3.6}$$

where (X_I, Y_I) are the receiver initial coordinates, and (X_n, Y_n) refer to the transmitter coordinates. Because the navigation frame was chosen to be centered at the receiver initial position this simplifies the equation to

$$R_{I,n} = \sqrt{(X_n)^2 + (Y_n)^2} \tag{3.7}$$

R_n can also be found using the formula [8]

$$R_n = \sqrt{(X_n - X_i)^2 + (Y_n - Y_i)^2} \tag{3.8}$$

where (X_i, Y_i) refer to the receiver coordinates at the time the measurement was taken. Note that in a perfect system with no errors (X_i, Y_i) is the state X and Y of the Kalman filter. Equations (3.7) and (3.8) can then be substituted into equation (3.5) yielding

$$\Delta R = \sqrt{(X_n)^2 + (Y_n)^2} - \sqrt{(X_n - X_i)^2 + (Y_n - Y_i)^2} \tag{3.9}$$

It is evident because of the quadratic and square root portions of ΔR that this equation is non-linear. The measurement model in equation (2.24) must be used. Taking the partial derivative of equation (3.9) yields an H matrix of the form

$$H = \begin{pmatrix} 0 & 0 & 0 & \frac{X_1 - \hat{X}}{\sqrt{(X_1 - \hat{X})^2 + (Y_1 - \hat{Y})^2}} & \frac{Y_1 - \hat{Y}}{\sqrt{(X_1 - \hat{X})^2 + (Y_1 - \hat{Y})^2}} \\ 0 & 0 & 0 & \frac{X_2 - \hat{X}}{\sqrt{(X_2 - \hat{X})^2 + (Y_2 - \hat{Y})^2}} & \frac{Y_2 - \hat{Y}}{\sqrt{(X_2 - \hat{X})^2 + (Y_2 - \hat{Y})^2}} \\ \vdots & \vdots & \vdots & \vdots & \vdots \\ 0 & 0 & 0 & \frac{X_n - \hat{X}}{\sqrt{(X_n - \hat{X})^2 + (Y_n - \hat{Y})^2}} & \frac{Y_n - \hat{Y}}{\sqrt{(X_n - \hat{X})^2 + (Y_n - \hat{Y})^2}} \end{pmatrix}$$

The final piece needed to perform the measurement update step is the covariance of the measurement R. Typically this is always assumed to be AWGN added to the measurement, but in this case the only noise that affects the measurement is added to the OFDM signal directly. Because simulations average over multiple symbols the effect of this noise at higher SNR values does not impact the actual measurement

taken therefor this noise is not used in the calculation of the R matrix. The error that does affect the measurement comes from the fact that the TDOA measurements are not exact and can only be as accurate as the resolution defined by the sampling frequency. This means that a sampling frequency of 20 MHz yields a sample resolution of approximately 15 meters, and a sampling frequency of 300 MHz yields a sample resolution of approximately 1 meter.

When a measurement is taken the actual measurement must lie between the measurment taken and the next measurement posible. This distribution is assumed to be linear between the measurements and thus its variance can be calculated as the variance of a uniform distribution using the formula found in [13]

$$\sigma^2 = \frac{1}{12}\left(a - b\right)^2 \qquad (3.11)$$

where a and b are any two consecutive possible measurements. Therefor with a sampling frequency of 20 MHz and measurement resolution of 15 meters the variance would be $\sigma^2 = \frac{15^2}{12}$ and with a sampling frequency of 300 MHz and measurement resolutin of 1 meter the variance would be $\sigma^2 = \frac{1^2}{12}$. Because all transmitters are considered independent of each other, all TDOA measurements are independent yielding

$$R = \begin{pmatrix} \sigma^2 & 0 & \cdots & 0 \\ 0 & \sigma^2 & \cdots & 0 \\ \vdots & \vdots & \ddots & \vdots \\ 0 & 0 & \cdots & \sigma^2 \end{pmatrix}$$

3.6 Adding Noise

Initial simulations assumed a perfect channel. In reality this is not the case, and in fact there will be noise added to the signal. To simulate this AWGN was added to the OFDM signals. A wide range of *Signal to Noise Ratios* (SNR) were examined.

3.7 Adding Multipath

Noise is not the only thing that can affect TDOA accuracy. Although OFDM signals are designed to combat the effects of multipath, it may still cause incorrect TDOA measurements. The TDOA measurement works under the assumption that the *Line of Sight* (LOS) path magnitude of the signal is higher than any non LOS path. Typically this is true, but in an urban situation where many reflections and path interferences are common it is possible for a non LOS path signal to become stronger than the LOS signal. In order to simulate these effects a virtual water tower was added to the simulation. The OFDM signals would reflect off the water tower and be received at the receiver with a time delay based on the additional signal travel time it took for the signal to reach the tower, and reflect to the receiver. The magnitude of this reflection was modeled as a two dimensional random variable with a Ricean distribution with a *Probability Density Function* (PDF) [13]

$$p_R\left(r\right) = \frac{r}{\sigma^2} e^{-\left(r^2 + s^2\right)/2\sigma^2} I_0\left(\frac{rs}{\sigma^2}\right), r \geq 0 \tag{3.13}$$

where $R = \sqrt{X_1^2 + X_2^2}$ and $s^2 = m_1^2 + m_2^2$. X_1 and X_2 are statistically independent Gaussian random variables with means m_1 and m_2 and common variance σ^2. For this research $m_1 = 0.33$, $m_2 = 0$, and $\sigma^2 = 0.0625$ ralative to a unit-magnitude LOS path. The position of the water tower is shown in figure 3.3.

Once the delay amount and reflection magnitude were calculated, a channel model for each signal was convolved with the signal received by the receiver. This essentially introduced a multipath reflection with a random magnitude and phase.
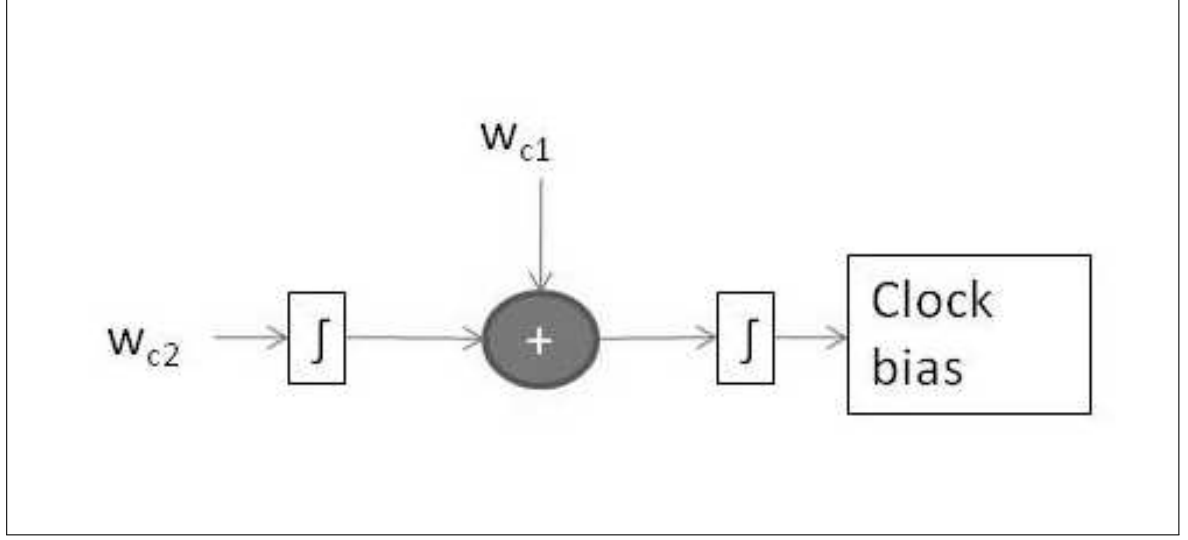
Figure 3.4:   Model used to represent GPS clock

3.8   Adding Clock Errors

Systems using time measurements for navigation are suseptible to large error in position due to clock errors. Because the signals travel at the speed of light, a small error in timing can cause a large error in calculated distance and thus in position. To see these effects, clock errors were introduced to the transmitters. The model used was that typically used for modeling GPS clocks and is shown in Figure 3.4 [3]. w_{c1} and w_{c2} are independent zero mean white Gaussian noise sources with variances equal to 0.036 $\frac{m^2}{s^2}$ and 0.141 $\frac{m^2}{s^4}$ respectively.

To simulate the effects of the errors the OFDM signals were circshifted additionally by the amount of error induced by the clock. This will cause inaccurate TDOA measurements. In order to combat these effects a reference receiver was introduced. The reference receiver did not move. It used the same OFDM signals as the mobile. Because there was no movement by the reference, the circshift amount was based only on the clock errors. An actual TDOA of the mobile receiver could then be calculated by

$$TDOA_{actual} = TDOA_{mobile} - TDOA_{reference} \qquad (3.14)$$

Note that because the reference is calculating a time difference, and is not moving; the initial position does not need to be known. The reference can be stationed anywhere as long as it does not move. Also note that the signal from the reference is not used in any cross-correlations; only the clock data is used.

IV.   Results and Analisys

This chapter details results from the simulations described in Chapter 3. Section 4.1 illustrates correct operation of the Kalman filter as well as effects of the number of transmitters and oversampling of the transmitters. Section 4.2 discusses the RMS errors over time comparing the TDOA aided systems to a system using only an INS. Section 4.3 illustrates the effects of AWGN when added to the OFDM signals, while Section 4.4 discusses the effects of multipath reflections on the system. Finally Section 4.5 details the effects of clock errors on the system and a mitigation technique for these errors. Table 4.1 outlines the figures in this chapter including their parameters and metrics.

Table 4.1:   Table of experiments

Figure	TX	Samp Freq (MHz)	Noise	Multipath	clock err	Metric (m)
4.1	3	20	No	No	No	X & Y errors
4.2	3	300 (oversampled)	No	No	No	X & Y errors
4.3	1	20	No	No	No	X & Y errors
4.4	1	300	No	No	No	X & Y errors
4.5	3	20 & 300	No	No	No	RMS error
4.6	1	20 & 300	No	No	No	RMS error
4.7	3	20 & 300	Yes	No	No	Average error
4.8	3	20	No	2-Ray	No	X & Y errors
4.9	3	300	No	2-Ray	No	X & Y errors
4.10	3	20	No	2-Ray	No	X & Y errors
4.11	3	300	No	2-Ray	No	X & Y errors
4.12	3	20	No	2-Ray	No	X & Y errors
4.13	3	300	No	2-Ray	No	X & Y errors
4.14	3	20 & 300	No	No	Yes	RMS error
4.15	3	20 & 300	No	No	Yes w Ref	RMS error

4.1   Effects of the Number of Transmitters and Oversampling

The purpose of the first set of simulations was to ensure that the TDOA computation algorithm was working properly, and to ensure the Kalman filter was working properly as well. These simulations also investigated the effects of oversampling the OFDM signal as well as the effects of using multiple OFDM transmitters as opposed
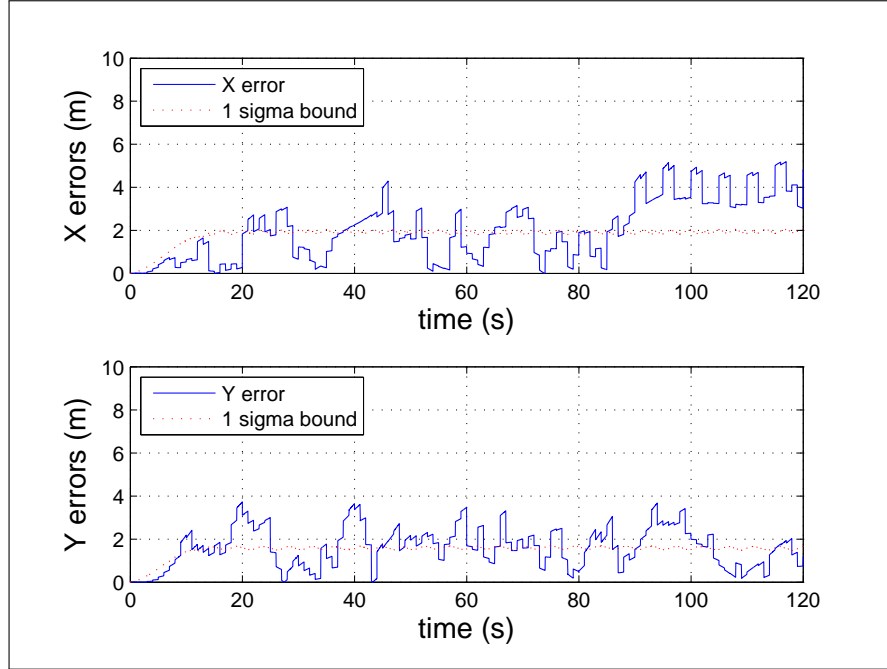
Figure 4.1:   X and Y errors versus time compared to one standard deviation of the errors for three transmitters with a 20 MHz sampling frequency.

to a single OFDM transmitter. This simulation used a perfect channel with no noise or infinite SNR. There were also no multipath effects or clock errors incorporated into the simulation. To ensure the Kalman filter was working properly, a plot of the X and Y position errors over time were plotted along with the filter estimated standard deviation of those errors over time. The filter estimated standard deviation of these errors was obtained by taking the square root of the diagonal entries in the P matrix at each time instant calculated using equations (2.16) and (2.21). If the errors in position are within one standard deviation approximately 66 % of the time then the filter is working properly. If position errors frequently lie far outside one standard deviation then the filter may not be operating properly. The error plots for three transmitters using both 20 MHz and 300 MHz sampling frequencies are shown in Figures 4.1 and 4.2, respectively. The error plots for one transmitter using both 20 MHz and 300 MHz sampling frequencies are shown in Figures 4.3 and 4.4, respectively.

Several things can be noted from Figures 4.1 through 4.4. The first of which is that errors using three transmitters are much smaller than those from using only one
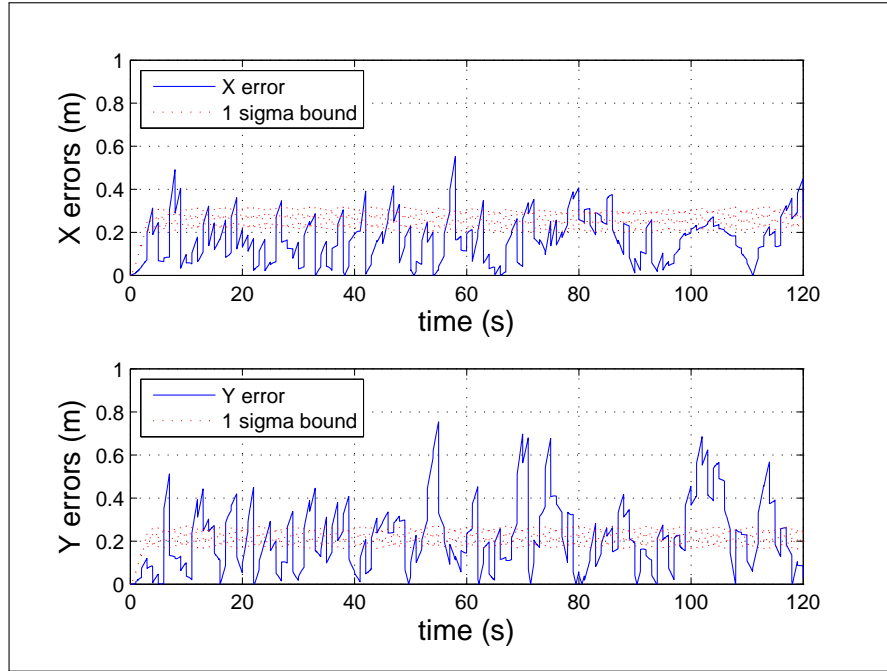
35

Figure 4.2: X and Y errors versus time compared to one standard deviation of the errors for three transmitters with a 300 MHz sampling frequency.
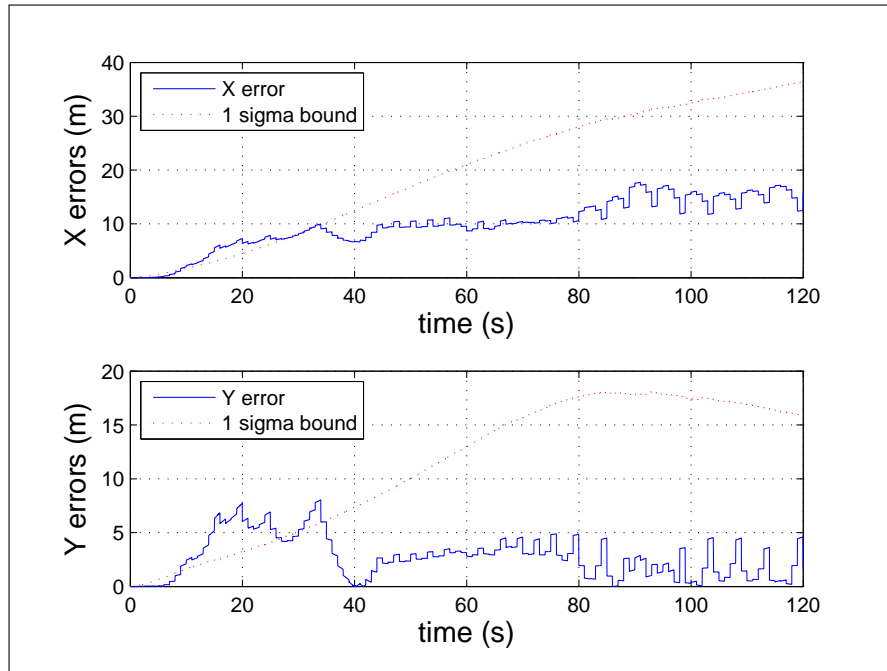

Figure 4.3: X and Y errors versus time compared to one standard deviation of the errors for one transmitter with a 20 MHz sampling frequency.
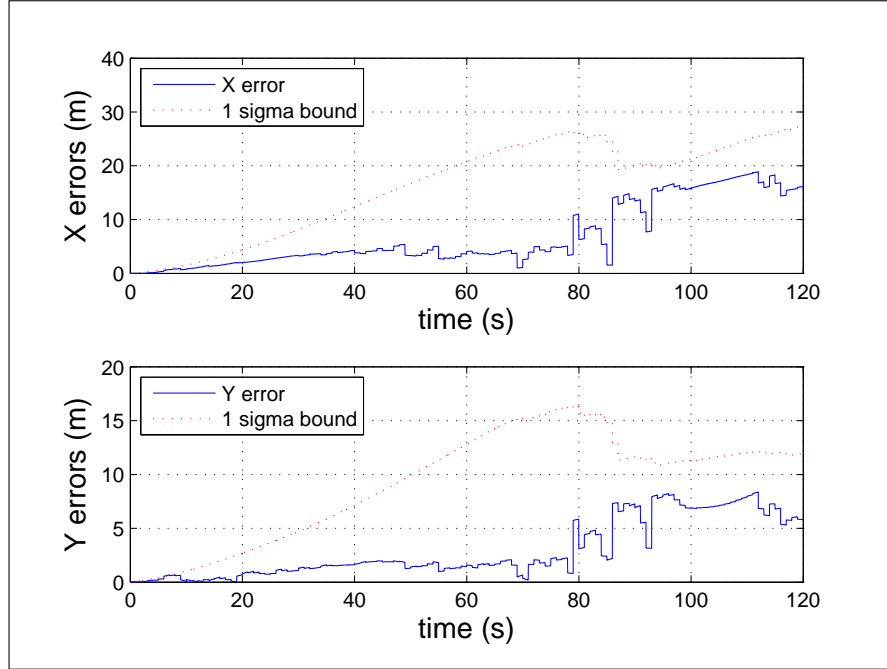
Figure 4.4: X and Y errors versus time compared to one standard deviation of the errors for one transmitter with a 300 MHz sampling frequency.

transmitter. This is expected because more transmitters provide more measurements. More measurements provide more information to the Kalman filter. More information to the filter yields a more accurate position estimate, and a more accurate position estimate means smaller error. The second thing that can be noticed (more so from the three transmitter plots) is that oversampling the OFDM signals provides smaller errors. Oversampling of the OFDM signal provides for a finer TDOA measurement, meaning this measurement can be much more precise. A more precise measurement gives better information to the Kalman filter and thus a better position estimate can be obtained. Note however, that this oversampling assumes all errors in the OFDM signal are independent. If oversampled too much, an actual system may start to have time-correlated errors which could degrade performance.

4.2 RMS Error Versus time

The next set of simulations used one and three transmitters at both 20 MHz and 300 MHz sampling frequencies. Again no multipath effects, noise or clock errors
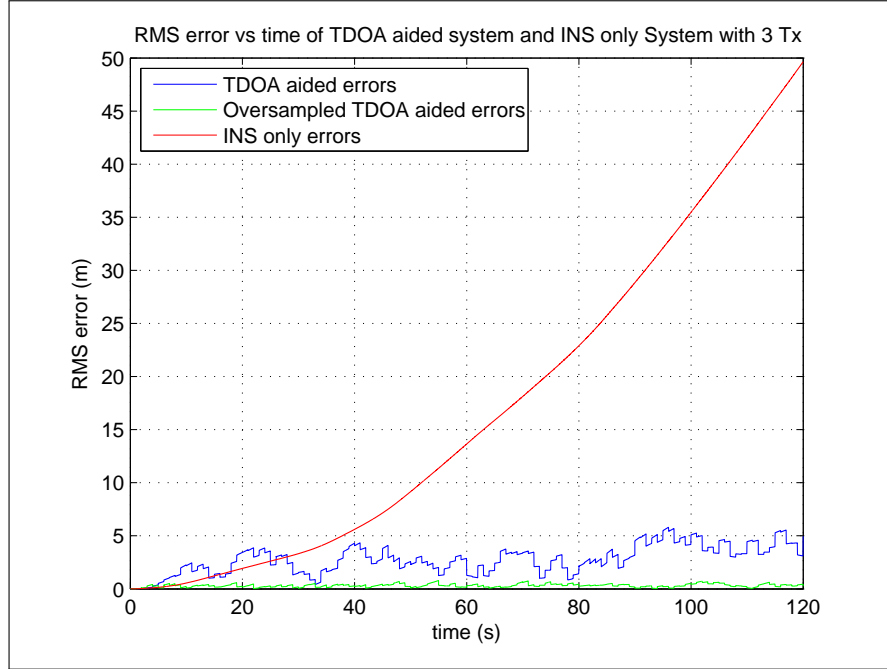
37

Figure 4.5: RMS error with 3 transmitters. The above simulations were run 10 times each and RMS errors were calculated.

were added. All four simulations were run ten times with ten different realizations of noise on the INS measurements. The object was to compute the *Root Mean Square* (RMS) error over time for each system and compare it to the error when only the INS system was used without TDOA aiding. This will allow the accuracy of the aided system to be compared to the INS only over time. RMS error for each time instance i was calculated using the formula

$$E_{RMSi} = \sqrt{\frac{1}{10} \sum_{k=1}^{10} \left(\hat{X}_{ki} - X_{Ti} \right)^2 + \left(\hat{Y}_{ki} - Y_{Ti} \right)^2} \qquad (4.1)$$

where (X_{Ti}, Y_{Ti}) is the truth reference position at each time instance i, and k refers to the kth run of the simulation. RMS errors for the three transmitter system are shown in Figure 4.5 and RMS errors for the single transmitter system are shown in Figure 4.6.
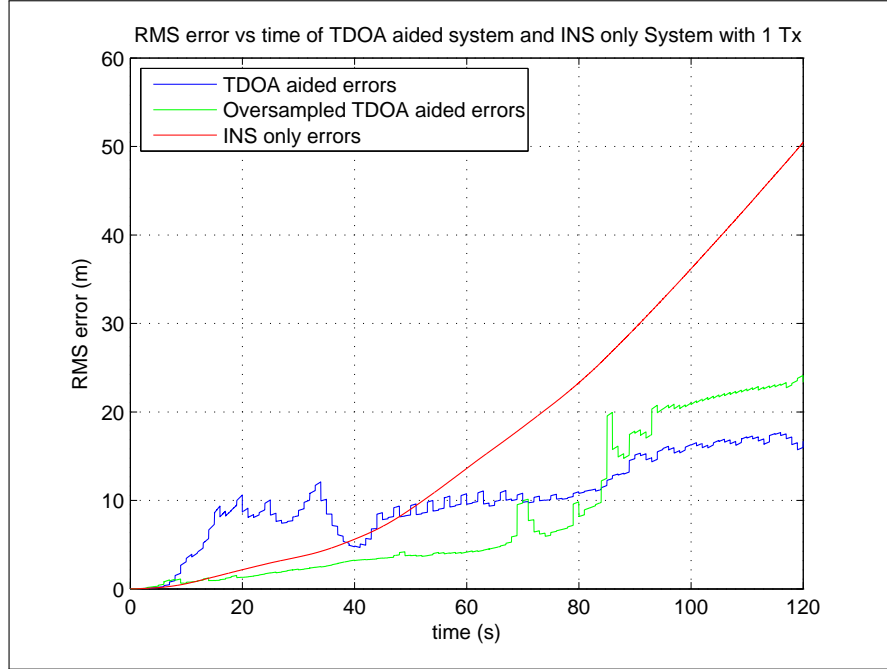
Figure 4.6: RMS error with 1 transmitter. The above simulations were run 10 times each and RMS errors were calculated.

Because measurements taken by an INS are integrated twice, errors in the measurements tend to grow over time. This error can potentially grow without bound as seen in Figures 4.5 and 4.6. Aiding the INS with the TDOA measurements keeps the errors bounded as can be seen from the Figures. Also, again when looking at the errors in Figure 4.5 It is clear that oversampling with more than one transmitter can provide better position accuracy.

4.3 Effects of Noise

The next set of simulations incorporated AWGN added to the OFDM signal. No multipath effects or clock errors were introduced to the system. This test sought to attain the breaking point of the system in terms of noise. This simulation used SNR values ranging from -40 dB to +10 dB. This test used three transmitters with sampling frequencies of 20 MHz and 300 MHz. The average error over time for each SNR value was calculated and plotted versus SNR. This is shown in Figure 4.7.
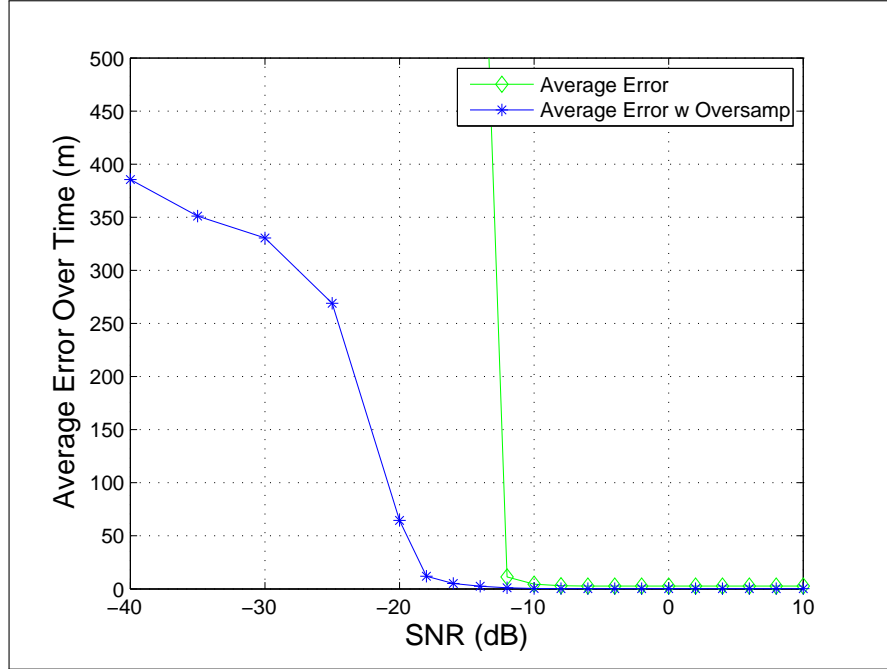
Figure 4.7: Average error over time versus SNR. The TDOA system does not produce accurate TDOA estimates at SNR values lower than -10 dB.

Figure 4.7 shows that at approximately -10 dB the noise added to the OFDM signal becomes too strong, and the TDOA system cannot calculate a correct TDOA. The oversampled system continues to work at a slightly smaller SNR value. This limit could possibly be decreased if the number of symbols averaged over were increased. However, if increased too much the TDOA would not be constant over the symbols, and this could decrease accuracy.

4.4 Effects of Multipath

To investigate the effects of multipath, simulations using three transmitters at sampling frequencies of 20 MHz and 300 MHz were run. These simulations incorporated the multipath model presented in Section 3.7. These simulations were run without noise or clock errors so that all effects could be attributed to multipath. A plot of X and Y errors versus time for the 20 MHz simulation is shown in Figure 4.8. A plot of X and Y errors versus time for the 300 MHz simulation is shown in Figure 4.9.
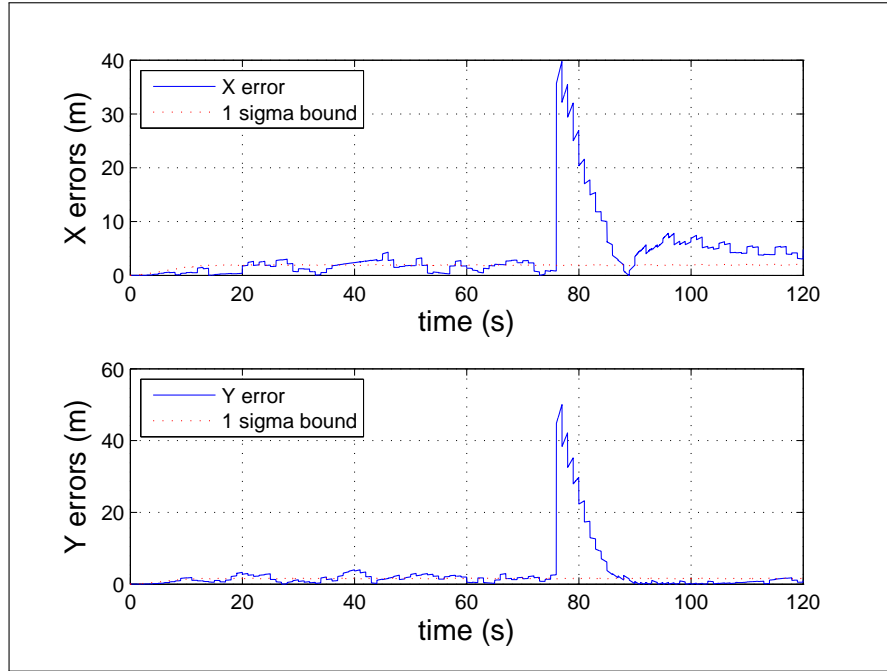
Figure 4.8: X and Y errors versus time for the 20 GHz simulation. Multipath effects cause large errors in the position solution.
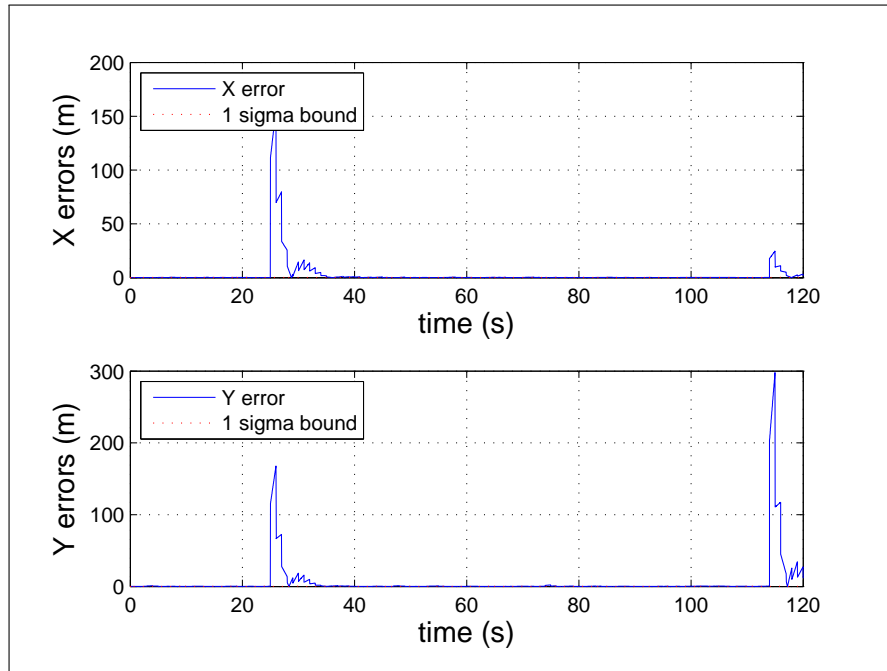

Figure 4.9: X and Y errors versus time for the 300 GHz simulation. Multipath effects cause large errors in the position solution.
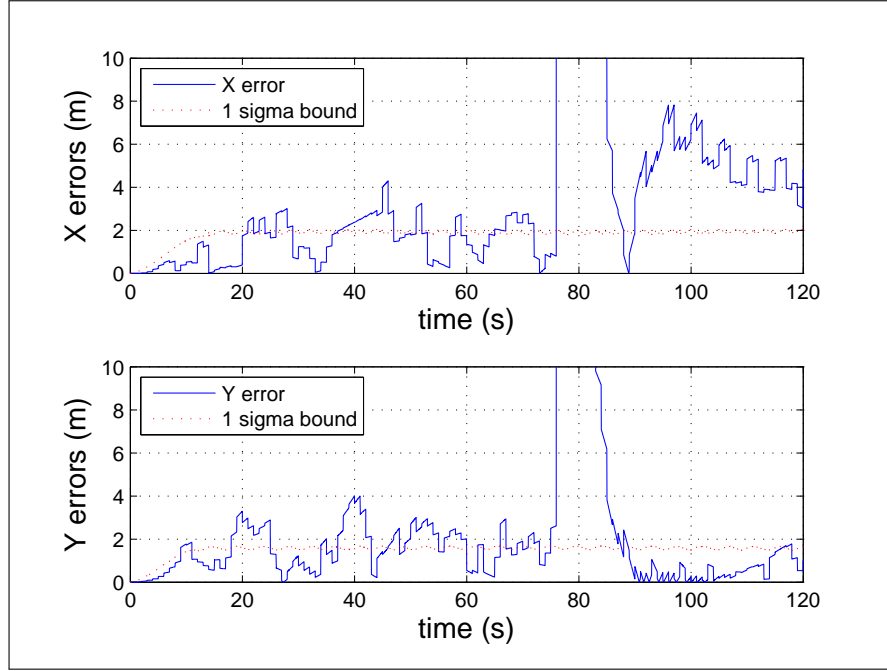
Figure 4.10: Zoomed in X and Y errors versus time for the 20 GHz simulation. Multipath effects cause large errors in the position solution.

In Figure 4.8 a large increase in the error magnitude occurs at time $T = 76$. This error occured when the randomly generated magnitude of the multipath reflection was greater than the magnitude of the line of sight path. This caused an incorrect TDOA measurement to be taken. This faulty information input to the Kalman filter caused large position errors. Comparing Figures 4.8 and 4.9 also shows that when errors due to multipath occur in an oversampled system, the resulting position errors are larger than those in a less frequently sampled system. They also tend to correct themselves quicker once correct measurements are taken. Note the fact that some of the multipath reflections were at delays longer than the CP length. In OFDM communication systems bit errors due to multipath cannot be corrected if the delay is longer than the CP length. Because this system does not decode the transmitted bits this longer delay does not cause a problem. Figures 4.10 and 4.11 show a zoomed in version of Figures 4.8 and 4.9. These plots show that the system is working correctly until the multipath reflection is higher than that of the LOS path.
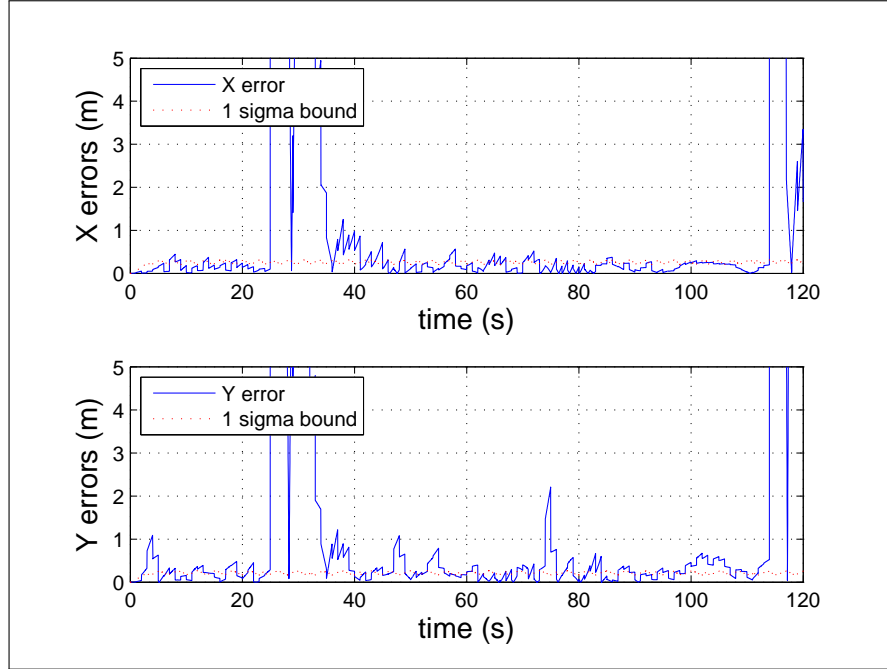
Figure 4.11:   Zoomed in X and Y errors versus time for the 300 GHz simulation. Multipath effects cause large errors in the position solution.

In a normal system that uses only a TDOA measurement to obtain position there would be no way to know if an error due to multipath occured, and thus no way to correct the position error. However, because an INS is being combined with the TDOA using a Kalman filter a technique called residual monitoring can be used to combat these effects. While operating the Kalman filter computes the difference in the actual measurement and the predicted measurement. This value is known as the residual. If this value is extremely high an error has typically occured. A simulation was run monitoring the residual. If the residual was higher than three times the TDOA resolution (i.e. 45 m for the 20 MHz sampled system and 3 m for the 300 MHz sampled system) the Kalman filter would disregard the measurement and essentially only propogate the state estimate instead of using the measurement update step. Results from these simulations are shown in Figures 4.12 and 4.13.

By monitoring the residuals inside the Kalman filter large errors due to multipath effects are able to be mitigated. The filter recognizes the presence of a bad
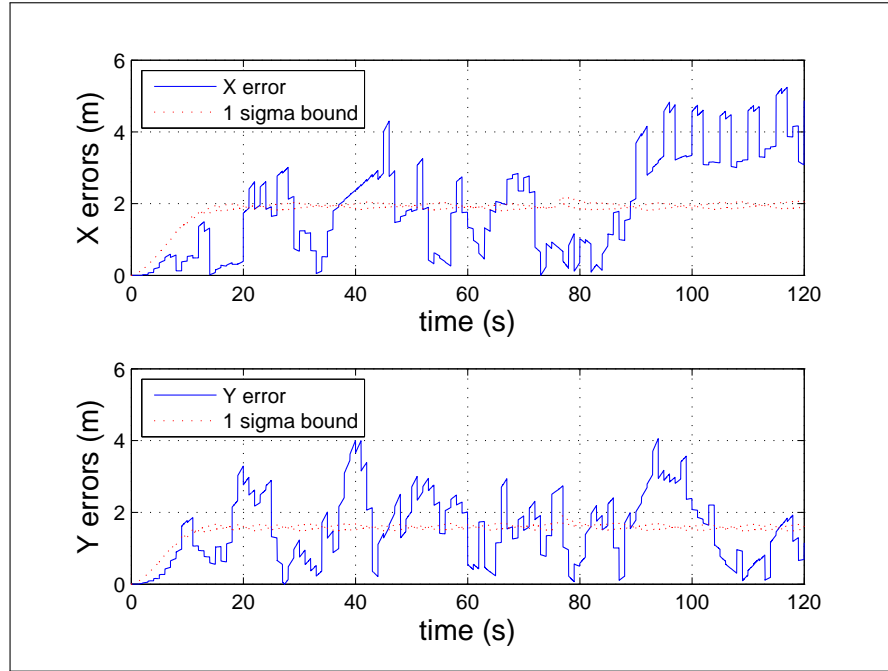
Figure 4.12: X and Y errors versus time for the 20 GHz simulation. Residual Monitoring can combat the effects of multipath reflections.
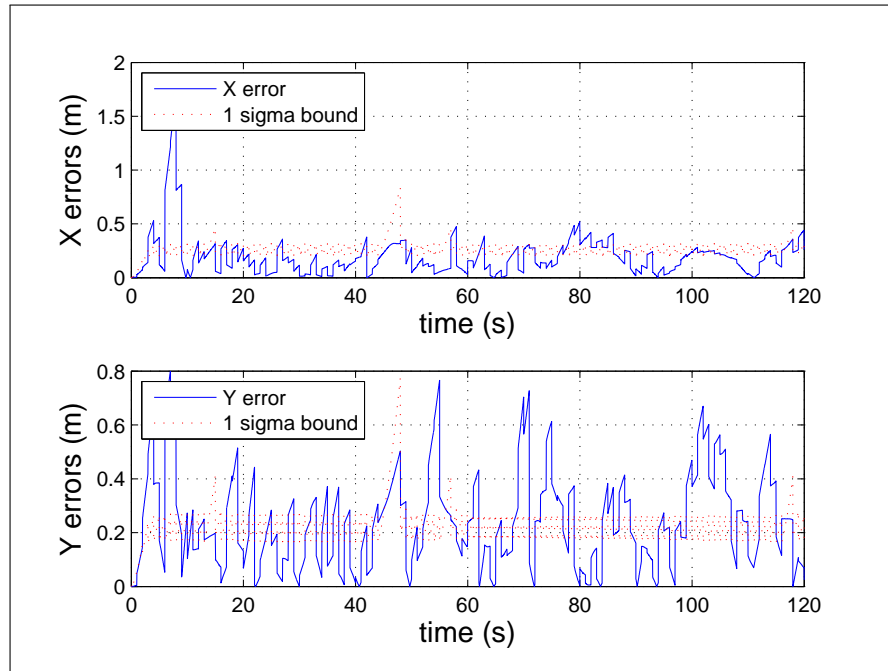

Figure 4.13: Zoomed in X and Y errors versus time for the 300 GHz simulation. Residual Monitoring can combat the effects of multipath reflections.

measurement and does not use the measurement and will propogate the system until the next measurement occurs.

4.5   Effects of Clock Errors

To investigate the effects of clock errors on the system, simulations using three transmitters at both 20 MHz and 300 MHz sampling frequencies were run. These simulations incorporated the clock errors without a reference receiver described in Section 3.8. This simulation was run without multipath or noise errors so that all effects could be attributed to the clock errors. Each simulation was run ten times and the RMS error versus time was computed. This can be seen in Figure 4.14. Note that the clock errors only affect the transmitter clocks. Receiver clock errors were not introduced because they can be estimated in a way similar to what is done in current GPS systems, i.e. included as an additional variable in the state vector.

Because the clock errors driven by noise are integrated twice, this produces an accuracy drift similar to that of the INS sytem. Because of this the same unbounded error drift behavior is seen. In order to combat this drift a reference receiver was added to the system. This system used the same OFDM signals as the mobile receiver. The reference receiver did not move and therefor any TDOA measurement taken was the result of transmitter clock drift. The reference TDOA measurement was then sent to the mobile receiver at every time a measurement was taken or once per second. From observing the effect of clock errors in Figure 4.14 clock errors grow much quicker than errors from the INS. Because of this the reference TDOA measurement should be used each time a mobile TDOA measurement is taken. If not the errors from the transmitter clocks could be larger than those using only the INS. Then by using equation (3.14) a true TDOA measurement could be calculated. The previous simulation was run using the reference system and results are shown in Figure 4.15.

Figure 4.15 shows that using a reference receiver can negate the effects of clock errors in the system. By comparing Figure 4.15 to Figure 4.5 the system works as good as it did when no clock errors were introduced.
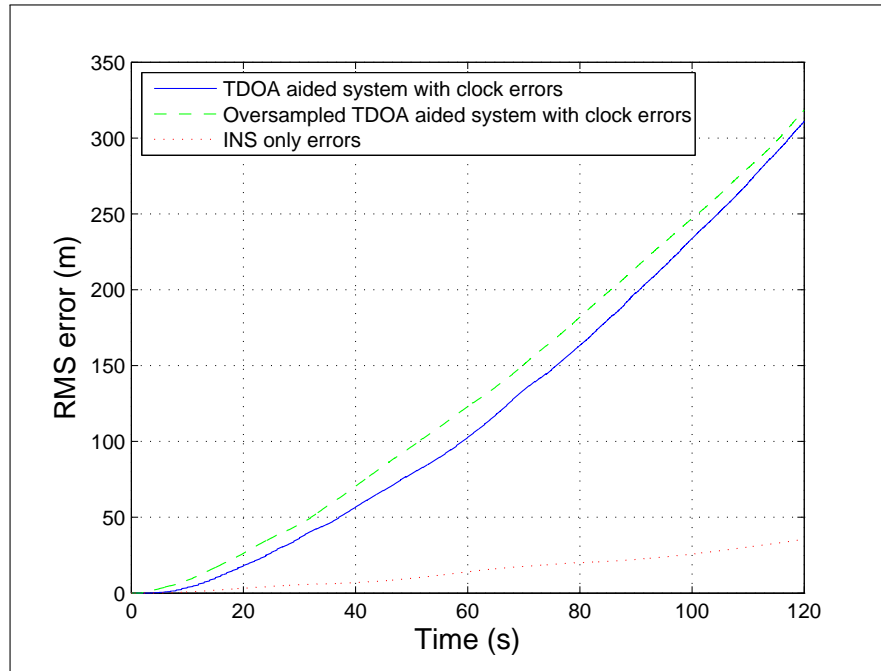
Figure 4.14:   RMS errors over 10 runs versus time for both 20 MHz and 300 MHz sampling frequencies. Clock errors have been introduced and cause the error to grow over time.
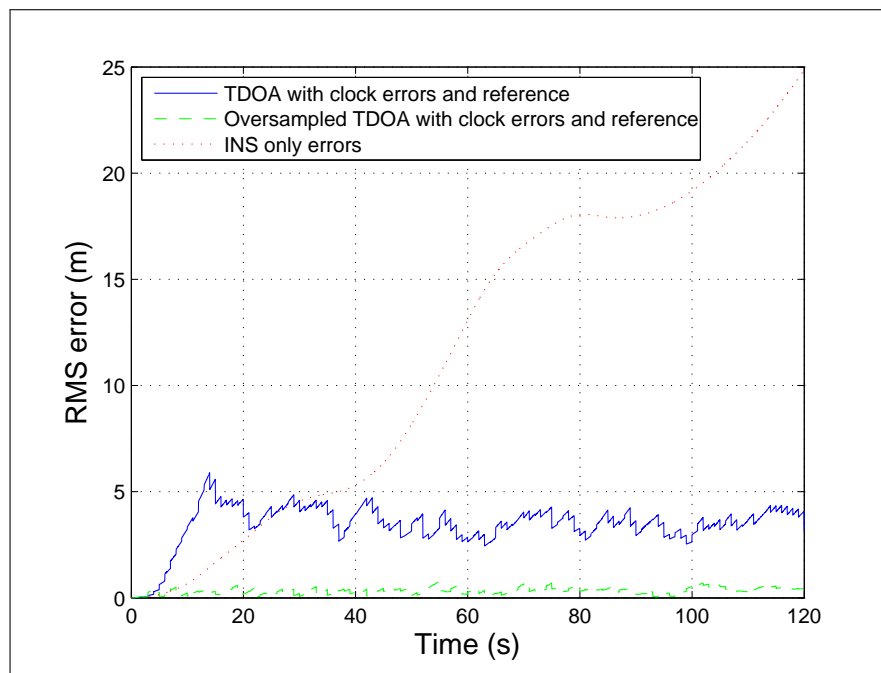

Figure 4.15:   RMS errors over 10 runs versus time for both 20 MHz and 300 MHz sampling frequencies. Reference receiver has been added to correct clock errors.

V. Conclusions and Future Work

This Section details conclusions that were drawn from the results of this research. Future research potential is also presented here.

5.1 Conclusions

First it can be noted that this system works in simulation. OFDM signals of opportunity can be used to aid an inertial navigation system. The position accuracy of a TDOA aided system is much better than that of an INS only system. The system also benefits from the use of more transmitters. It is expected that adding more than three transmitters may increase the position accuracy even more. Also it has been shown that oversampling the OFDM signals will result in an increase of position accuracy.

Several potential causes of error were investigated. The effects of noise were found to be negligable at higher SNR values, while the system does not work at SNRs lower than -10 dB. Multipath errors were also found to be negligable unless the multipath reflection magnitude was greater than the LOS magnitude.

Finally the effects of clock errors were investigated. The GPS quality clock errors showed an even larger increase in errors than the INS. If unmitigated these errors would cause very large position errors. A reference receiver was used to mitigate these errors. The reference receiver was used to calculate a self TDOA in the same was as the mobile receiver. This TDOA measurement was then sent to the mobile to update the clock error of the system. No cross correlation techniques for calculating TDOAs were used. With the use of the reference receiver position accuracy was shown to be approximately the same as when no errors were introduced.

5.2 Future Work

The first area of future work should include the use of multiple mobile receivers to mitigate clock errors instead of one dedicated reference receiver. It has been hy-

pothesized that if more transmitters were used that multiple mobile receivers could cooperatively estimate transmitter clock errors.

Next a more realistic INS model should be investigated. The INS model used in this research was very simplified and did not take into account effects of gravity and Earth rotation. An actual hardware INS system could also be used to take actual INS measurements. Differential GPS could be used as a truth reference, and the OFDM signal of opportunity TDOA measurements could be simulated in a similar way. To do this an INS capable of measureing specific force and angular rate in three dimensions would be needed. They system would also need to be equiped with a differential GPS system to be used as a truth reference. Matlab could then be used to simulate the TDOA measurements in a manner similar to that used in this research. A more rigorous Kalman filter could then use the simulated measurements to aid the INS.

Finally once more realistic INS simulations are conducted, a receiver capable of using OFDM signals for TDOA measurements should be investigated. This would allow for a full hardware system to be used. This hardware system would give a better idea of the position accuracy that could be expected in an actual fielded system. This system would use the previous stated equipment in addition to a receiver capable of receiving OFDM signals and performing the TDOA measurements. The transmission source would need to be an actual OFDM signal. WiFi could be used for indoor tests or another OFDM source such as satelite radio ground stations or clearwire could also be used.

Bibliography

1. Institute of Electrical and Electronics Engineers. Piscataway, NJ. *IEEE Std 802.11-2007, IEEE Standard for Information technology-Telecommunication and information exchange between systems-Local and metropolitan area networks-Specific requirements, Part 11: Wireless LAN Medium Access Control (MAC) and Physical Layer (PHY) Specifications: Chapter 17. Orthogonal Frequency Division Multiplexing (OFDM) PHY specification for the 5 GHz band.* 2007.

2. Van de Beek J, M Sandell and P Borjesson. "ML Estimation of Time and Frequency Offset in OFDM Systems". *IEEE Transactions on Signal Processing*, 45(7):1800–1805, July 1997.

3. Brown, R and P Hwang. *Introduction to Random Signals and Applied Kalman Filtering.* John Wiley & Sons, New York, 1997. ISBN 0-471-12839-2.

4. Burr, A. "The Multipath Problem: An Overview". *IEE Colloquium on Multipath Countermeasures.* London, UK, May 1996.

5. Caffery, J Jr. and C Stuber. "Overview of Radiolocation in CDMA Cellular Systems". *IEEE Communications Magazine*, 36(4):38–45, April 1998.

6. Eggert, R. *Evaluating the Navigation Potential of the National Television System Committe Broadcast Signal.* Master's of Science, Air Force Institute of Technology, 2950 Hobson Way, WPAFB, OH 45433-7765, March 2004.

7. Einstein, A. *Relativity: The Special and General Theory.* Henry Holt, New York, NY, 1920.

8. H Bang, G Jee S Kim S You S Kong H Jung M Hyun J Kim, J Lee. "Location Determination in Wireless OFDM System". *ION GNSS 18th International Technical Meeting of the Satellite Division.* Long Beach, CA, September 2005.

9. Kim, B. *Evaluating the Correlation Characteristics of Arbitrary AM and FM Radio Signals for the Purpose of Navigation.* Master's of Science, Air Force Institute of Technology, 2950 Hobson Way, WPAFB, OH 45433-7765, March 2006.

10. Maybeck, P. *Stochastic Models Estimation and Control, Vol I.* Academic Press Inc., Orlando, FL, 1979.

11. McEllroy, J. *Navigation Using Signals of Opportunity in the AM Transmission Band.* Master's of Science, Air Force Institute of Technology, 2950 Hobson Way, WPAFB, OH 45433-7765, September 2006.

12. Misra, P and P Enge. *Global Positioning System: Signals, Measurements, and Performance.* Ganga-Jamuna Press, Lincoln, MA, 2001. ISBN 0-9709544-0-9.

13. Proakis, J. *Digital Communications.* McGraw-Hill, New York NY, 4th edition, 2001. ISBN 0-07-232111-3.

14. Sklar, B. *Digital Communications: Fundamentals and Applications.* 15. Prentice Hall PTR, Second edition, December 2006. ISBN 0-13-084788-7.

15. Titterton, D and J Weston. *Strapdown Inertial Navigation Technology.* Peter Peregrinus Ltd., Lavenham, UK, 1997. ISBN 0-86341-260-2.

16. Velotta, J. *Navigation Using Orthogonal Frequency Division Multiplexed Signals of Opportunity.* Master's of Science, Air Force Institute of Technology, 2950 Hobson Way, WPAFB, OH 45433-7765, September 2007.

17. Veth, M and J Raquet. "Alignment of Optical and Inertial Sensors Using Stellar Observations". *Proceedings of ION GNSS 2005.* September 2005.

18. W Henkel, P Odling P Borjesson, G Taubock and N Petersson. "The Cyclic Prefix of OFDM/DMT - An Analysis". *2002 International Zurich Seminar on Broadband Communications. Access, Transmission, Networking.* Zurich, Switzerland, February 2002.

19. Wikipedia. "Orthogonal Frequency-Division Multiplexing — Wikipedia, The Free Encyclopedia", 2009. [Online]. Available at http://en.wikipedia.org/wiki/OFDM. [Accessed 20-January-2009].

20. Zou, W and Y Wu. "COFDM: An Overview". *IEEE Transactions on Broadcasting*, 41(1):1–8, March 1995.

REPORT DOCUMENTATION PAGE

Form Approved
OMB No. 0704–0188

1. REPORT DATE (DD–MM–YYYY)	2. REPORT TYPE	3. DATES COVERED (From — To)
26–03–2009	Master's Thesis	Sept 2007 — Mar 2009

4. TITLE AND SUBTITLE

Fusion of Inertial Sensors and
Orthogonal Frequency Division Multiplexed (OFDM)
Signals of Opportunity
for Unassisted Navigation

5a. CONTRACT NUMBER

5b. GRANT NUMBER

5c. PROGRAM ELEMENT NUMBER

6. AUTHOR(S)

Jason Crosby, Captain, USAF

5d. PROJECT NUMBER

ENG09-182

5e. TASK NUMBER

5f. WORK UNIT NUMBER

7. PERFORMING ORGANIZATION NAME(S) AND ADDRESS(ES)

Air Force Institute of Technology
Graduate School of Engineering and Management (AFIT/EN)
2950 Hobson Way
WPAFB OH 45433-7765

8. PERFORMING ORGANIZATION REPORT NUMBER

AFIT/GE/ENG/09-11

9. SPONSORING / MONITORING AGENCY NAME(S) AND ADDRESS(ES)

Jacob L. Campbell
Air Force Research Lab, AFMC
2241 Avionics Circle, Bldg 620
Wright-Patterson AFB, OH, 45433-7301
DSN: 785-6127 x4154
jacob.campbell@wpafb.af.mil

10. SPONSOR/MONITOR'S ACRONYM(S)

AFRL/RYRN

11. SPONSOR/MONITOR'S REPORT NUMBER(S)

12. DISTRIBUTION / AVAILABILITY STATEMENT

APPROVED FOR PUBLIC RELEASE; DISTRIBUTION UNLIMITED.

13. SUPPLEMENTARY NOTES

14. ABSTRACT

The advent of the global positioning system (GPS) has provided worldwide high-accuracy position measurements. However, GPS may be rendered unavailable by jamming, disruption of satellites, or simply by signal shadowing in urban environments. Thus, this thesis considers fusion of Inertial Navigation Systems (INS) and Orthogonal Frequency Division Multiplexed (OFDM) signals of opportunity (SOOP) for navigation. Typical signal of opportunity navigation involves the use of a reference receiver and uses time difference of arrival (TDOA) measurements. However, by exploiting the block structure of OFDM communication signals, the need for the reference receiver is reduced or possibly removed entirely. This research uses a Kalman Filter (KF) to optimally combine INS measurements with the OFDM TDOA measurements. A proof of concept in two dimensions is shown, and effects of the number of transmitters, sampling rate, multipath, and clock errors are investigated.

15. SUBJECT TERMS

Orthogonal Frequency division Multiplex, Signals of Opportunity, Navigation, Inertial Navigation

16. SECURITY CLASSIFICATION OF:			17. LIMITATION OF ABSTRACT	18. NUMBER OF PAGES	19a. NAME OF RESPONSIBLE PERSON
a. REPORT	b. ABSTRACT	c. THIS PAGE			Richard K. Martin, Civ, USAF, (ENG)
U	U	U	UU	64	19b. TELEPHONE NUMBER (include area code) (937) 255–3636, x4625; Richard.martin afit.edu

Standard Form 298 (Rev. 8–98)
Prescribed by ANSI Std. Z39.18